Phosphorus cycling by stream biofilms exposed to continuous and episodic loading patterns

by

Christine Lundsgaard-Nielsen

A thesis

presented to the University of Waterloo

in fulfillment of the

thesis requirement for the degree of

Master of Science

in

Biology

Waterloo, Ontario, Canada, 2023

Author’s Declaration

I hereby declare that I am the sole author of this thesis. This is a true copy of the thesis, including any required final revisions, as accepted by my examiners.

I understand that my thesis may be made electronically available to the public.

Abstract

Anthropogenic activities have led to nutrient enrichment of streams, causing eutrophication of water bodies on a global scale. Eutrophication is frequently tied to an excessive influx of phosphorus (P); a crucial nutrient that often limits productivity in freshwater ecosystems. Strategies for tackling eutrophication increasingly rely on watershed models, which predict when and how much P is carried from land to water bodies. However, some watershed models overlook the in-stream cycling of P, potentially hindering eutrophication management by miscalculating P loads to waterbodies. Stream biofilms may play an important role in P cycling through P retention and transformation. However, understanding of these processes within biofilms is limited, particularly in the context of continuous (i.e., point source) and episodic (i.e., non-point source) P delivery patterns to streams.

To address the knowledge gap in P cycling by stream biofilms, I investigated the potential of stream biofilms to act as P sinks and reactors under continuous and episodic loading patterns. This was achieved through a 25-day experiment in artificial streams using three treatment levels of soluble reactive phosphorus (SRP) loading: 1) unenriched – a constant 10 µg P/L concentration; 2) episodically enriched – a constant 10 µg P/L concentration with a 48-hour pulse of 400 µg P/L; and 3) continuously enriched – a constant 40 µg P/L concentration. The study aimed to compare patterns of P transformation, retention, and uptake amongst these loading patterns.

Results showed that approximately 15% of the SRP load was retained within the biofilm across all loading patterns. 75% of the SRP load was transformed into different P forms under unenriched and continuously enriched patterns. In contrast, the episodically enriched biofilms transformed 60% of the SRP load. The biofilms' ability to transform and uptake P decreased during the second day of the pulse, suggesting that the extended duration and high concentration of the pulse overwhelmed the biofilms in the episodic loading pattern.

Stream biofilms demonstrated potential to act as both P reactors and P sinks and may help to delay P loads and reduce P bioavailability in downstream ecosystems. However, the ability of stream biofilms to transform P delivered in an episodic loading pattern may be reduced compared to continuous loading patterns, depending on the concentration and duration of the pulse. Maximizing P transformation by stream biofilms could involve delivering P in a continuous rather than an episodic loading pattern where feasible. Integrating biofilm P cycling into watershed models could prove beneficial, but its impact might vary depending on modeled time scales and P species. This research

highlights the influence of biofilms on nutrient dynamics in stream ecosystems and emphasizes the need for their inclusion in ecosystem management strategies.

Acknowledgements

Firstly, I would like to thank my supervisor, Adam Yates, for his invaluable guidance, expertise, and enthusiasm towards research throughout my degree. I am grateful for the opportunity to work under your mentorship. Thank you to my committee members, Helen Jarvie and Josh Neufeld, who generously provided ideas and feedback.

I would like to acknowledge the hard work of my collaborators Chris Parsons, Sebastian Lingertat, and Zoey Duggan from the Watershed Hydrology and Ecology Research Division at Environment and Climate Change Canada, who provided funding and technical assistance.

Thank you to Philippe Van Cappellen and Marianne Vandergriendt for the use of lab space and technical assistance.

I would like to thank Edward Krynak, for the support during the various stages of this project, especially through the long hours at TRESS scraping biofilms. Your knowledge and dedication were crucial to the experiment's success.

Thank you to Nolan Pearce, for providing guidance throughout this endeavor.

I would also like to extend my appreciation to the City of London and the Upper Thames Region Conservation Authority for their support and permission to conduct research within their jurisdiction.

To my friends in the StrEAMS lab, thank you for being there through the highs and lows, for celebrating successes and providing reassurance during setbacks.

Lastly, I could not have undertaken this journey without the support of my friends, my family, Jerusan, and Miso.

Table of Contents

List of Figures

List of Tables

List of Abbreviations

AFDM	Ash-Free Dry Mass
DGT LSNP-NP	Diffusive Gradients in Thin Films for Phosphate in Solution
DI	Deionized
GLM	General Linear Model
H_2SO_4	Sulfuric Acid
HCl	Hydrochloric Acid
ICP-OES	Inductively Coupled Plasma Optical Emission Spectroscopy
KH_2PO_4	Potassium Dihydrogen Phosphate
N	Nitrogen
NH_4NO_3	Ammonium Nitrate
NLET	National Laboratory for Environmental Testing
NO_3	Nitric Acid
P	Phosphorus
SRP	Soluble Reactive Phosphorus
TN	Total Nitrogen
TP	Total Phosphorus

Chapter 1
Introduction and literature review

1.1 Introduction and problem statement

Anthropogenic activities have led to nutrient enrichment of streams, accelerating eutrophication of waterbodies worldwide (Smith, 2003). Eutrophication can be defined as increased primary productivity in water due to a surplus of nutrients (Correll, 1999). Ecosystem degradation caused by eutrophication threatens public health, fisheries, and recreation (Chislock et al., 2013), prompting an urgent need to improve approaches to eutrophication management (Jenny et al., 2020). Eutrophication is often linked to excess phosphorus (P) loading (Findlay & Kasian, 1987), as P is the primary limiting nutrient in many freshwater ecosystems (Correll, 1999). Management of eutrophication is increasingly being informed by watershed models that predict the timing and amount of P loads from land to receiving waters and effects of management actions (Jarvie et al., 2012).

Some widely used watershed models, such as the Export Coefficient Model, assume that P loads to a body of water are equal to the sum of P loads output from each source in its catchment (Ding et al., 2010). But, studies have shown that P loads entering streams are not equal to those measured at the outlet, likely due to within-stream P retention (Withers & Jarvie, 2008). It is estimated that within-river retention can reduce P loads in large rivers by up to 68% (Jarvie et al., 2012). Thus, it is likely that streams behave as active reactors, rather than passive pipes as some models assume (Casas-Ruiz et al., 2017). Models that do not accurately calculate P inputs to downstream ecosystems due to lack of consideration of in-stream P retention may incorrectly predict the effects of management practices and impede the mitigation of eutrophication (Withers & Jarvie, 2008).

The lack of incorporation of in-stream P retention into P export models may be due to an absence of suitable model coefficients arising from a poor understanding of how in-stream P cycling influences P export. Both abiotic stream components, such as stream bed sediments, and biotic stream components, such as biofilms, can cycle P (Jarvie et al., 2005). Stream biofilms, also termed periphyton, are diverse assemblages of autotrophs (algae, bacteria) and heterotrophs (bacteria, fungi) embedded in an extracellular matrix and adhered to benthic substrates (Lock et al., 1984). Stream biofilms can cycle P loads via uptake (sorption of P onto the biofilm surface or into the biofilm) (Price & Carrick, 2014), assimilation (integration of P into biomass) (Riegman & Mur, 1984),

transformation (change in P species) (Pearce et al., 2023), and retention (storage of P over a period of time) (Jarvie et al., 2012). These P cycling processes by biofilms can contribute to the self-purification of streams and have even been applied in wastewater treatment (Craggs et al., 1996). However, knowledge of these processes is limited, especially in the context of the spatially and temporally dynamic pathways by which P is delivered to streams.

The timing and source of P loadings to streams could influence the amount of P cycling by stream biofilms. Delivery of P loads to streams can range from continuous to episodic patterns, typically depending on whether the P source is point (e.g., wastewater treatment facility) or non-point (e.g., agricultural lands), respectively (Withers & Jarvie, 2008). It was previously believed that stream biofilms cannot effectively assimilate episodic P loads, based on the hypothesis that episodic loads are of short duration resulting in P bypassing biofilms (Stamm et al., 2014). However, recent experiments have shown that biofilms can assimilate both continuous and episodic P loads (Davies & Bothwell, 2012; Pearce et al., 2020). Despite these studies, the amount that stream biofilms may influence P export under different loading patterns has not been quantified. Therefore, the goal of my thesis is to quantify the potential of stream biofilms to transform and retain continuously and episodically delivered P loads. Knowledge P cycling by stream biofilms is an important step towards improving watershed models and effectively using the self-purification services that streams provide (Zhao et al., 2019).

1.2 Literature review

1.2.1 Sources of phosphorus to streams

Sources of P to streams can vary depending on the surrounding land use (Chen et al., 2016). Natural sources of P to streams include the weathering of calcium phosphate rich rock, atmospheric deposition, terrestrial organic matter, and groundwater (Gardner, 1990). Streams in undisturbed areas generally have low P concentrations because P release from natural sources, such as by weathering, is slow (Shen et al., 2011). In contrast, streams impacted by anthropogenic activities typically have higher P concentrations (Sonoda et al., 2001). In areas with a high proportion of agricultural land, chemical phosphate fertilizer, livestock waste, and septic tank systems are common sources of P (Mainstone & Parr, 2002; Richards et al., 2016). In urbanized areas, municipal and industrial wastewater, pet waste, and lawn fertilizer are common sources of P (Brett et al., 2005; Drolc & Zagorc Koncan, 2002).

The P source affects the delivery pattern of P, causing variability in the temporal and spatial patterns of loads reaching streams (Mainstone & Parr, 2002). Point sources of P are derived from discrete locations, such as effluent outfalls from wastewater treatment facilities (Brett et al., 2005). Point sources normally release enriched P loads with low temporal variability that are independent of runoff, causing a continuous pattern of P delivery to streams. In summer when low flows result in less dilution, point sources can disproportionately increase P concentrations in receiving streams (Bowes et al., 2008). Non-point sources are derived from diffuse areas, such as excess phosphate fertilizer applied to agricultural fields. Non-point sources generally result in short duration, high concentration P loads that peak during periods of high runoff (Jarvie et al., 2006), leading to episodic delivery patterns (Zięba & Wachniew, 2021). Streams that receive P from non-point sources typically have increasing P concentration with increasing river flow (Bowes et al., 2008).

1.2.2 P cycling by stream biofilms

Once P enters a stream it has various fates in the aquatic environment, moving between compartments and changing form as it travels downstream (Newbold et al., 1983). The cycling of nutrients while they are carried downriver is also called nutrient spiralling (Newbold et al., 1983). Both abiotic and biotic stream compartments can cycle P, leading to the transient storage and transformation of P (Stutter et al., 2010). For example, accumulation of P in abiotic stream compartments, such as benthic sediments, has been found to modulate P export from streams (Dorioz et al., 1989). Uptake of P by stream sediments has been studied extensively and rates up to 160 mg P /m^2/day have been reported (Dieter et al., 2015; Haggard & Sharpley, 2006; Tiessen et al., 1989; Withers & Jarvie, 2008). The role of biotic stream compartments in P cycling is not as well studied.

Biotic stream P compartments include benthic biofilms, phytoplankton, macrophytes (House, 2003), zooplankton, macroinvertebrates, and larger consumers such as fish (McIntyre et al., 2008). Biofilms are ubiquitous in streams and their importance in P cycling is increasingly recognized (Dodds, 2003; Vymazal, 1988). Biofilms have been reported to uptake up to 72 mg P /m^2/day (Parker et al., 2018; Williamson et al., 2016). Biofilms are genetically diverse, multitrophic level communities (Bengtsson et al., 2018), and thus have several mechanisms of P uptake. Both autotrophic and heterotrophic microorganisms primarily take up P from the water column, but can also obtain P from benthic sediment (Lu et al., 2016). Additionally, autotrophic microorgnisms can cause increases in pH during photosynthesis that favors P precipitation at the biofilm surface (Jarvie

et al., 2002; Neal, 2001). Heterotrophic microorganisms can also uptake P from trapped particulate material and detritus (Suberkropp & Chauvet, 1995).

P uptake by biofilms can be influenced by environmental conditions, which can be divided into physical (e.g., light, temperature, flow) and chemical (e.g., nutrient availability, pH) stream characteristics. Environmental conditions can influence biofilm P uptake rates indirectly by altering biomass, since higher amounts of biofilm biomass may take up P more rapidly (Sabater et al., 2002), and by changing the community composition of the biofilm, since P affinity and uptake mechanisms vary with the types of cells in the biofilm (Jansson, 1988; Steinman & Duhamel, 2017; Yao et al., 2011). Environmental conditions can also influence biofilm P uptake directly by altering P uptake kinetics (Balik et al., 2021).

Physical parameters such as light, flow velocity, physical disturbance, temperature, substrate size, and water residence time can alter P uptake by biofilms. Physical disturbance, such as by grazers or scouring, can influence P uptake by stream biofilms through changes in biomass (Mulholland et al., 1983; Price & Carrick, 2013). P uptake can also vary with substrate type, since different substrate sizes can have variable amounts of surface area available for biofilm colonization (Hanrahan et al., 2018; Lottig & Stanley, 2007). Temperature can play a role in biofilm metabolism and biomass (Delgado et al., 2017), and therefore may change P uptake rates by biofilms. Changes in light availability, due to variations in canopy cover or turbidity, can also control biofilm assimilation, and potentially P uptake, due to stimulation of photosynthesis (Schiller et al., 2007). Flow velocity can have a subsidy-stress effect on stream biofilm growth and P uptake (Biggs et al., 1998). If biofilms are not adapted to high flow velocities, sloughing can occur. However, higher flow velocity can also facilitate P uptake by renewing P supply to cells (Craggs et al., 1996). Water residence time may also alter uptake rates by changing the exposure time of the biofilm to P (Feijoó et al., 2011).

Chemical characteristics of the stream such as the ambient P concentration, form of P present, and pH can alter P uptake by biofilms. Biofilms are able to take up P passively during periods of high P concentration and actively during periods of low P concentration (Jansson, 1988). P uptake rate typically increases with ambient P concentration, as per the Michaelis-Menten equation used in enzyme kinetics (Steinman & Duhamel, 2017). However, uptake may reach a maximum at high P concentrations (Pearce et al., 2023). Some forms of P, such as soluble reactive phosphorus (SRP), are readily available for biofilm uptake while other forms, such as organic and particulate P, can become

available through decomposition and cleavage. SRP is easiest for biofilms to take up because SRP does not require hydrolysis of phosphate ester bonds via phosphatase before uptake (Jansson, 1988; Steinman & Duhamel, 2017). However, biofilms can also take up other forms of P, such as dissolved organic P (Nausch et al., 2018). Biofilm biomass can be correlated with stream pH (Bayer et al., 2021), and therefore may influence P uptake rates. It is important to control these environmental factors when studying P uptake by biofilms (Beck & Hall, 2018).

Uptake and assimilation of P by stream biofilms may result in P being stored in a reach, changing the timing and amount of P travelling downstream (Matheson et al., 2011). After uptake, P can be integrated into structural elements (e.g., nucleic acids or phospholipids) to drive cell growth (Lu et al., 2014), stored in a labile pool within cells, and stored within the extracellular matrix of the biofilm (Borovec et al., 2010). Through the storage of P, stream biofilms may act as transitory P sinks. Few studies have been conducted on retention of P by biofilms and therefore there is a limited understanding of the environmental factors that may impact P retention by biofilms. However, one study showed that algae generally exhibit greater capacity to store nutrients than bacteria because of differences in cellular structures (Schade et al., 2011), and therefore the community composition of biofilms may influence retention. A second study found that the amount of time that P is retained may vary with temperature (Zhao et al., 2019). One study also hypothesized that periphyton can decrease stream flow, which may increase nutrient retention simply by increasing water retention time (Dodds, 2003).

Biofilms may transform P through the processes of uptake and assimilation, changing the form of P travelling downstream (Meyer & Likens, 1979). Over time, portions of the biofilm may detach (Graba et al., 2012), releasing P as particulate organic P into the water column (Nausch et al., 2018). Senescence may cause cells to lyse and release P as dissolved organic P such as nucleic acids (Nausch et al., 2018) or unreactive P such as polyphosphates (Pearce et al., 2023). P may also be cycled through different forms as it travels between cells within the biofilm (Jansson, 1988). Through the transformation of P, stream biofilms may act as P reactors (Casas-Ruiz et al., 2017). A previous study demonstrated that stream biofilms can transform SRP from the water column into polyphosphates, phosphomonoesters, and phosphodiesters (Pearce et al., 2023). Biofilms may change the bioavailability of P in downstream ecosystems by transforming SRP into less bioavailable forms (Reddy et al., 1999).

Previous studies have shown that P cycling by biofilms may adapt to continuous and episodic loading patterns. Biofilms have been shown to have increased P content during P pulses through in situ chamber and artificial stream experiments (Humphrey & Stevenson, 1992; Pearce et al., 2023; Rier et al., 2016). Studies also have found that benthic algal biomass accrual was comparable under continuous and episodic P loading patterns (Davies & Bothwell, 2012; Pearce et al., 2020). A recent artificial stream experiment found that biofilms transformed and assimilated P delivered in various pulse sizes (Pearce et al., 2023).

1.2.3 Benefits and limitations of biofilms studies in real and artificial streams

Studies in real and artificial streams have been widely used to examine stream biofilm structure and function (Battin et al., 2003; Pearce et al., 2020; Ren et al., 2020). An artificial stream is an experimental system which simulates natural streams under controlled conditions. Artificial streams are not designed to fully mimic nature, but instead aim to isolate fundamental processes in complex ecosystems (Jessup et al., 2004). Studies in real and artificial streams both have tradeoffs which are important to consider when designing experiments (Table 1.1).

Artificial streams can be limited on a spatial scale (Coelho et al., 2013). The benthic environment of real streams is spatially heterogenous, which creates patchiness in stream biofilm structure and function (Morin & Cattaneo, 1992; Price & Carrick, 2014). Artificial streams typically provide a confined and homogenous channel, limiting the spatial variability that biofilms experience. Thus, studying biofilms in artificial streams may not fully capture the spatial dynamics that occur in real systems, potentially limiting the generalizability of research findings.

Artificial streams can also have limitations on a temporal scale when compared to real streams. In real streams, biofilms experience temporal variations due to seasonal changes (Gautam et al., 2022). For instance, during periods of high rainfall, increased water flow can scour biofilms in some areas, which are later recolonized. This leads to a mosaic of biofilm succession throughout the stream (DeNicola et al., 2021). Long-term temporal variations are more challenging to simulate in artificial streams, so artificial streams may have a homogenous level of succession due to the lack of disturbances. The temporal dynamics not captured in artificial streams could lead to inconsistencies between results when comparing between real and artificial streams (Sagarin et al., 2016).

Artificial streams can be oversimplified, leading to a lack of realism when compared to field studies (Coelho et al., 2013). For example, the feasibility of incorporating multitrophic interactions is

limited in artificial stream studies, and therefore the impacts of grazers such as macroinvertebrates and fish on biofilms are difficult to study (Coelho et al., 2013). In contrast, multiple trophic levels are naturally present in real streams.

Artificial streams allow rigorous control of environmental conditions, enabling repetition of experimental treatments (Gelwick, F. P. & McIntyre, P. B., 2017) and consistent experimental conditions between treatments. Artificial streams provide the ability to apply precise treatment levels (Coelho et al., 2013), such as controlling the concentration of nutrients. These treatment levels can be easily replicated in artificial streams and provides low within group variation, which decreases experimental error (Filazzola & Cahill Jr, 2021). In contrast, direct replication is essentially impossible in real streams and within group variation is higher. It is also difficult to replicate environmental conditions between treatments in field studies, leading to confounding factors (Coelho et al., 2013). Artificial streams offer greater control over experimental conditions to enhance the reliability of research findings.

Table 1.1 Advantages and disadvantages of studies in artificial and real streams.

	Artificial Streams	**Real Streams**
Spatial scale	Limited	Wide
Temporal scale	Limited	Wide
Degree of realism	Low	High
Control over environment	High	Low

1.3 Research objectives

The goal of my thesis was to quantify the potential of stream biofilms to act as P reactors and P sinks under continuous and episodic P loading patterns. My goal was achieved by conducting a 25-day artificial stream experiment to establish P transformation and retention by biofilms under continuous and episodic loading patterns. This goal can be separated into three objectives:

1. Compare SRP export amongst loading patterns to determine if stream biofilms can act as P reactors under different loading patterns. I hypothesize that biofilms will transform the highest proportion of the SRP load in the unenriched loading pattern and biofilms will

transform the smallest proportion of the SRP load when it is delivered in an episodic loading pattern.

2. Compare biofilm total phosphorus (TP) content and TP export amongst loading patterns to determine if stream biofilms can act as P sinks under different loading patterns. I predict that unenriched biofilms will retain the highest proportion of the SRP load and episodically enriched biofilms will retain the smallest proportion of the SRP load.

3. Compare the pattern of SRP uptake rate and the concentration of TP in the biofilm amongst loading patterns to provide an understanding of the ecological processes driving among pattern differences in P retention and transformation. I hypothesize that biofilm P uptake will be greatest in the episodic loading pattern during the pulse and smallest in the unenriched loading pattern.

Chapter 2
Materials and methods

2.1 Experimental setup

An artificial stream experiment was conducted to establish stream P cycling by biofilms under continuous and episodic P loading patterns. Three P loading treatment levels were used: 1) unenriched - constant concentration of 10 µg P/L (0.323 µM) as SRP; 2) episodically enriched - constant concentration of 10 µg P/L as SRP with a 48-hour pulse of 400 µg P/L (12.9 µM) as SRP, and; 3) continuously enriched - constant concentration of 40 µg P/L (1.29 µM) as SRP. Each treatment level was replicated in three randomly assigned artificial streams. Cumulative P load at the end of the experiment was approximately 1 g, 4 g, and 4 g to the unenriched, episodically enriched, and continuously enriched patterns, respectively (Figure 2.1). P concentrations were chosen based on regional nutrient criteria (Chambers et al., 2012), previous artificial stream experiments (Pearce et al., 2020), and baseline and storm-event concentrations of streams in southern Ontario (Raney & Eimers, 2014; Williams et al., 2018). The unenriched loading pattern was a control treatment that represented regional streams minimally by anthropogenic activities. The continuously enriched loading pattern represented streams receiving loads primarily from points sources, whereas the episodically enriched loading pattern represented streams receiving loads primarily from non-point sources. The experiment was 25 days long. This length was chosen to avoid biofilm senescence while allowing adequate time for the biofilm to respond to the P loading patterns. The 48-hour P-pulse in the episodically enriched loading pattern began on day 8 and ended on day 10, which provided the biofilm with time to establish before the pulse and two weeks to respond to the pulse.

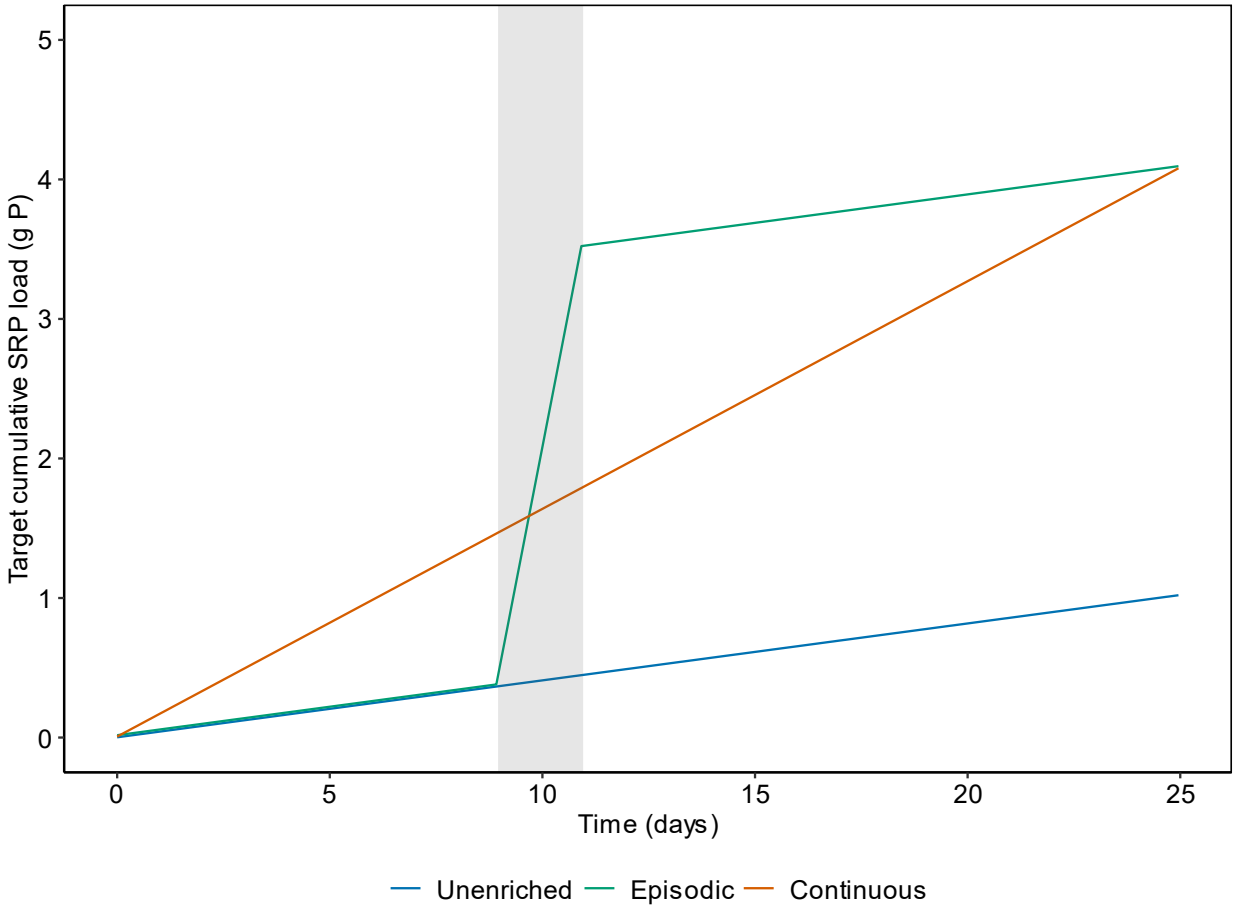

Figure 2.1 Target cumulative soluble reactive phosphorus (SRP) loads to artificial streams for unenriched, episodically enriched, and continuously enriched phosphorus (P) loading patterns over the 25-day experiment. Grey bar indicates duration of the pulse in the episodic loading pattern.

The artificial stream experiment was conducted at the Thames River Experimental Stream Sciences (TRESS) Center in London, Ontario from July 14 to August 8, 2022. The TRESS Centre is an outdoor facility with nine artificial streams (Figure 2.2a). Artificial streams at TRESS consist of sinuous channels that are 0.15 m deep, 0.2 m wide, and 7 m long (Figure 2.2b). The water depth was approximately 11 cm and each stream had a wetted surface area of 3.96 m^2. Low nutrient (TN = 406 µg/L and TP < 1 µg/L) water from the Lake Huron Water Supply system was used in the streams. Water was carbon filtered to remove chlorine prior to being added to the artificial streams.

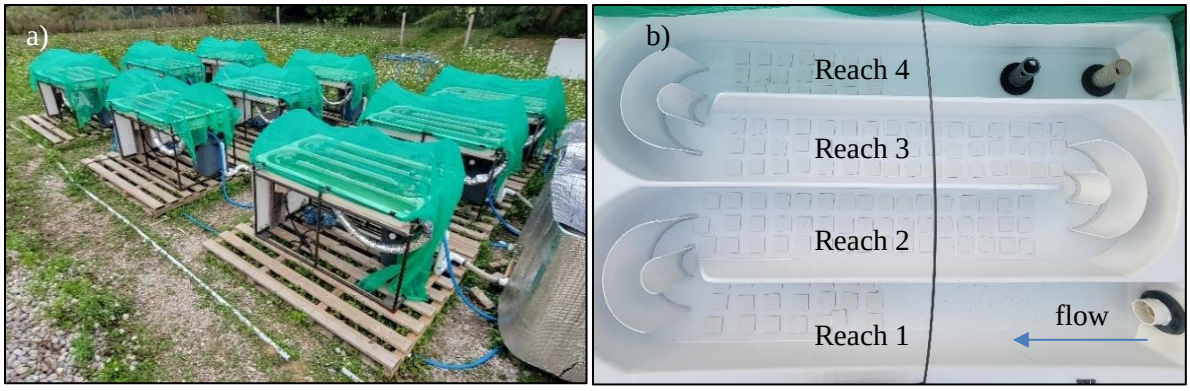

Figure 2.2 a) Photograph of the nine outdoor artificial streams at the Thames River Experimental Stream Sciences Centre. b) Top view of an artificial stream showing the white unglazed ceramic tiles, four reaches, and the direction of water flow (blue arrow).

One dosing pump was used to add a target baseline nitrogen (as NH_4NO_3) concentration of 1500 µg N/L and a target baseline SRP (as KH_2PO_4) concentration of 10 µg P/L from a 1000 L carboy to the common water supply. Individual diaphragm pumps delivered water to each stream from the common water supply. Additional SRP stored in two 1000 L carboys was delivered to each continuously and episodically enriched stream via individual dosing pumps that were connected to the outflow of each diaphragm pump. Flow rates of diaphragm and dosing pumps were calibrated daily to ensure nutrients were continuously delivered at the correct rates to maintain target nutrient concentrations. An impeller pump partially recirculated water and nutrients through each stream. Water had a residence time of approximately 2.5 hours.

N and SRP concentrations were confirmed before (SRP on day 1 and N on day 7), during (day 10), and after the pulse (day 24). A graduated cylinder was used to collect 4 L of water from the inflow tube of each stream to minimize the impact of individual nutrient pulses from the dosing pumps. A 45 mL subsample was taken from the graduated cylinder and the nitrogen concentration was confirmed using a portable spectrophotometer (Hach Canada, 2023a) following the TNT 835 protocol with a detection limit of 230-13500 µg/L (Hach Canada, 2023b). To confirm SRP concentrations, a 120 mL subsample was taken from the graduated cylinder and filtered (sterile cellulose acetate membrane, 0.45 µm) into a 125 mL glass bottle. SRP water samples were stored at 4 °C then shipped on ice to the National Laboratory for Environmental Testing (NLET) in Burlington, Ontario for SRP analysis (Environment and Climate Change Canada, 2018). SRP concentrations were measured using a standard molybdenum blue method via a colorimeter in a segmented continuous flow analyzer

(Environment and Climate Change Canada, 2019, 2020). The detection limit and expected error for SRP were 0.2 and 0.8 µg P/L for all water samples analyzed for SRP at NLET.

N concentrations were within 390 µg/L of the target. All nine streams were within 4.3 µg/L and 2.1 µg/L of the target SRP concentration ± expected error before and after the pulse, respectively (Figure 2.3). However, during the pulse, unenriched streams were between 6 to 9 ug/L below the target minus expected error, while continuously enriched streams were between 0.6 and 8.0 µg/L below the of the target concentration minus expected error and episodically enriched streams were ranged from 27 µg/L above and below the target concentration ± expected error. This deviation from the target could be due to low baseline P levels. SRP loads were calculated by multiplying flow by the target concentration and calculating the cumulative sum, but did not consider deviation from the target concentration.

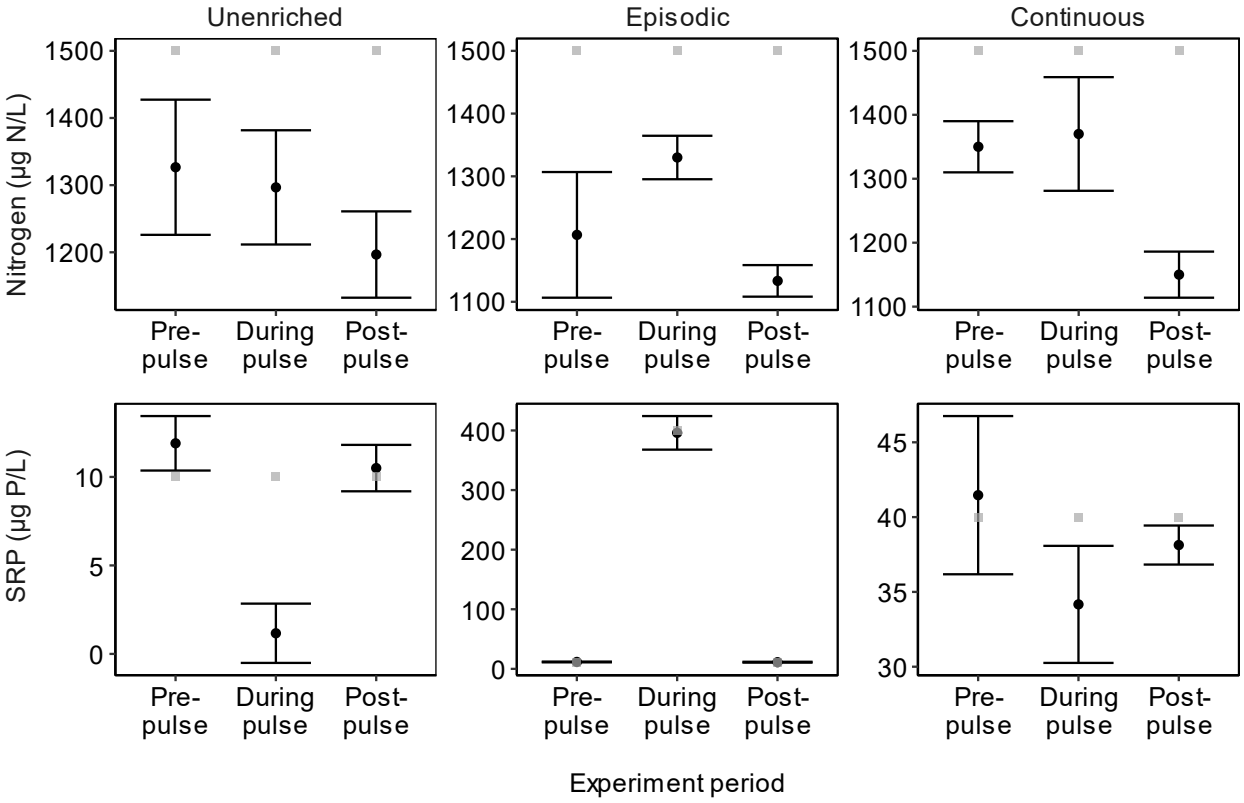

Figure 2.3 Average nitrogen (N) and soluble reactive phosphorus (SRP) concentrations (± one standard deviation) in the unenriched, episodically enriched, and continuously enriched loading patterns before, during, and after the phosphorus (P) pulse. Grey points represent target concentration.

Water temperature was recorded hourly using a HOBO Pendant logger (Onset's HOBO, 2023) placed in the second bend of each stream. Light availability was limited using a 50% shade cloth and two PAR loggers were placed under the shade cloths to record light availability at five-minute intervals. Water flow velocity was calibrated weekly using a water flow meter (OTT Hydromet, 2019). Besides SRP concentrations, physio-chemical conditions were consistent across all streams. Mean daily average water temperature was 21.87 ± 0.07 °C, degree days ranged from 566-573 °C, average daily photosynthetically active radiation under the shade cloths was 275.1 µmol/s/m^2, water flow velocity in the sampled reaches was 0.08 m/s, specific conductance was 242 S/m.

Square unglazed ceramic tiles (23.04 cm^2 each, Olympia Quebec 4.8 x 4.8 cm tile in Arctic White, Product # OD.QC.ARW.0202.FS) were added to each stream to provide a consistent surface for biofilm colonization. Unglazed tiles are commonly used as standardized substrate to reduce variability of biofilm growth (Price & Carrick, 2013). Tiles were only sampled from the second and third reaches because turbulence was high in the first reach. 48 tiles were placed in each of the second and third reaches (96 tiles total). Artificial streams were inoculated with biofilms collected from five local streams that spanned a gradient of P enrichment (Figure 2.4, Table 2.1). In each local stream, the biofilm from twenty randomly selected cobbles were scraped using a brush and rinsed using stream water into two 1 L Nalgene bottles. Large invertebrates were removed from the inoculum. Bottles from all streams were combined in a bucket, homogenized, and divided up into nine approximately 300 mL portions of inoculum. One portion of inoculum was poured into the first reach of each artificial stream, marking the start of the experiment.

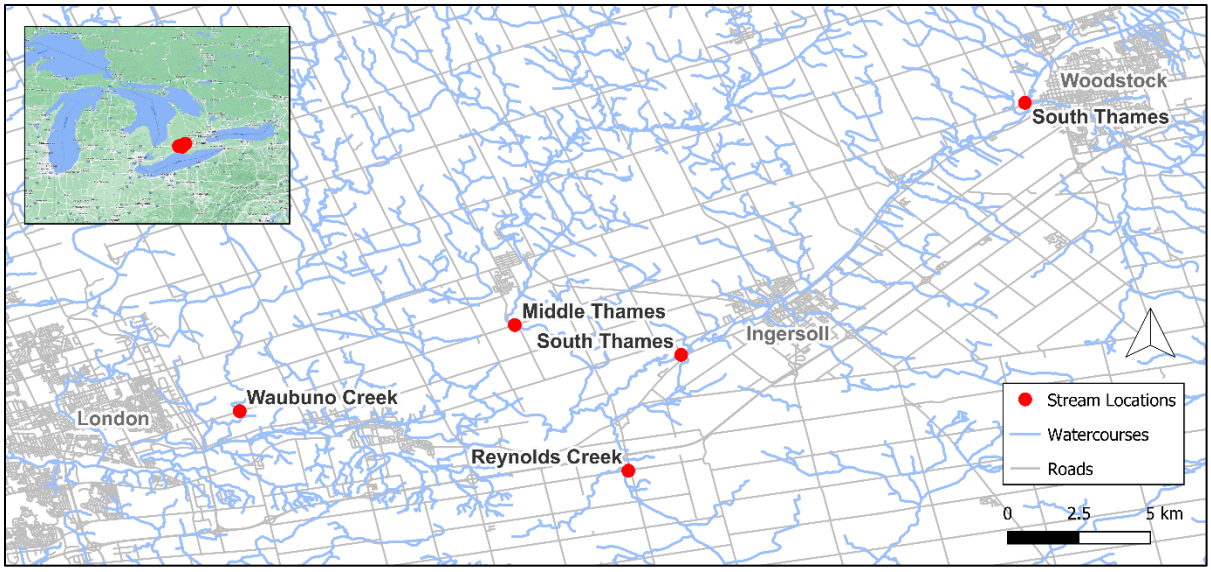

Figure 2.4 Map of five streams in Southern Ontario where inoculum was collected.

Table 2.1 Location, Strahler order, total phosphorus, and total nitrogen status of real streams used to inoculate artificial streams.

Stream Name	Location	Strahler Order	TP (mg/L)	TN (mg/L)
Waubuno Creek	42.994523, -81.116698	4	0.025	4.39
Reynolds Creek	42.969076, -80.949771	4	0.191	3.10
Middle Thames	43.031385, -80.998540	6	0.046	4.17
South Thames	43.018638, -80.92706	5	0.122	4.99
South Thames	43.126534, -80.779388	5	0.158	5.38

2.2 Sample collection and analysis

2.2.1 SRP export

SRP export from each stream was measured by deploying diffusive gradients in thin films (DGT) for phosphate in solution (LSNP-NP) passive samplers at the outflow of each stream for the entire duration of the experiment. The DGT LSNP-NP passive sampler functions by accumulating P on a ferrihydrite binding layer with a sampling area of 3.14 cm^2 after passage through a 0.14 mm polyethersulphone filter and a 0.8 mm hydrogel diffusion layer (DGT Research, 2023a). DGT passive samplers were installed at the outflow of each stream using fishing line threaded through the hole at the rim of the unit (Figure 2.5). The DGT passive samplers were replaced daily during the pulse in the

episodically enriched streams and twice throughout the experiment in the continuously enriched streams because the maximum load for a DGT passive sampler would have been exceeded in those loading patterns (Zhang et al., 1998). Passive samplers were also replaced in the unenriched streams at the beginning and end of the pulse to enable comparison with episodically enriched streams. Once removed, the passive samplers were rinsed with deionized water (DI) and stored in a clean plastic bag at 4 °C. The start and end time of deployment was recorded to the nearest minute for each passive sampler. For deployments of one day and seven days, the limits of detection are 0.07 and 0.01 µg/L P, respectively (Zhang et al., 1998).

DGT passive samplers were processed following the protocol described in manual by DGT Research (2023a). The DGT passive sampler was removed from the plastic bag and rinsed with DI water, then the binding gel layer was removed and placed in 5 mL of DI water. After one hour, the binding layer was placed in a clean sample tube and 5 ml of 0.25 M H_2SO_4 was added. The binding layer was left to sit fully immersed for 24 hours (DGT Research, 2023a). The solution was then analyzed using the colorimetric phosphate method based on molybdenum blue along with a set of six calibration standards (1, 2.5, 10, 25, 100, and 250 µg SRP/L). The detection limit for the molybdenum blue analysis was 1.62 µg SRP/L and the limit of quantification was 4.92 µg SRP/L. The time averaged concentration (*C*) of SRP in the outflow water was calculated using:

$$\text{Equation 1. } C = \frac{C_e * 5.2 * \Delta g}{D * A * t}$$

, where C_e is the measured concentration of analyte in the H_2SO_4 digestion , Δg is the thickness (cm) of the diffusive layer, D (cm^2/s) is the diffusion coefficient of SRP at the water temperature of deployment, A (cm^2) is the area of the exposure, and t (s) is the time of deployment (Mason et al., 2005). The average temperature during the deployment period for each DGT sampler was calculated using hourly water temperature and used to determine the corresponding diffusion coefficient (DGT Research, 2023b). Cumulative SRP export was determined by multiplying *C* for each deployment period by the flow of water out of the stream for each deployment period (i.e., 2.83 L/min), then calculating the cumulative sum. For plotting, cumulative standard deviation (*CSD*) was calculated using Equation 2:

$$\text{Equation 2. } CSD_{t_n} = \sqrt{{SD_{t_1}}^2 + {SD_{t_2}}^2 + \cdots + {SD_{t_n}}^2}$$

, where SD_{t_1} is the standard deviation of *C* during the first deployment period (Lindberg, 2000). The proportion of SRP not exported (%) was calculated by dividing cumulative SRP export by the cumulative SRP input from each stream, subtracting from 1, then multiplying by 100, as in Equation 3:

$$\text{Equation 3. SRP not exported} = 1 - \frac{SRP\ export}{SRP\ input} \times 100\%$$

The proportion of SRP associated with the pulse not exported (%) was also calculated using Equation 3, but SRP export was calculated by subtracting SRP export in the unenriched from the episodically enriched streams over day 8-10 and SRP input was calculated by subtracting SRP input to the unenriched from the episodically enriched streams over day 8-10.

Results from the DGT passive samplers were verified by measuring the SRP concentration of the water at the outflow of each stream using discrete samples. Water was sampled for SRP export after 6 days of growth (day 6), before the pulse (day 8), immediately after the pulse (day 11), on days 15 and 20, and on the last day of the experiment (day 25) for a total of six times (Table 2.2). For each sampling event, 120 mL of water was collected from the outflow of each stream (Figure 2.5). Water samples were refrigerated at 4 °C prior to being shipped on ice to NLET for SRP analysis. Cumulative SRP export was calculated by linearly interpolating TP concentration of the discrete samples between measurements, multiplying each concentration by the flow of water out of the stream for each time period, then calculating the cumulative sum. For plotting purposes, cumulative standard deviation was calculated using Equation 2.

Figure 2.5 Water sample (left) and DGT passive sampler (right) positioned at outflow of artificial stream.

2.2.2 Biofilm TP and biomass

Stream biofilms were sampled to determine biofilm TP content and biomass in each artificial stream on six occasions throughout the experiment: 1) after six days of growth (day 6); 2) before the pulse (day 8); 3) immediately after the pulse (day 11); 4) on day 15; 5) on day 20, and; 6) on the last day of the experiment (day 25) (Table 2.2). On each sampling occasion, three sets of three tiles (nine tiles total) were randomly selected from each stream. The biofilm from each set of tiles was scraped off the top surface of the tiles using a mini glass scraper and rinsed using carbon filtered water into a 120 mL specimen cup (n = 3, N = 27) (Figure 2.6). The remaining biofilm was then scoured using a toothbrush and again rinsed into the specimen cup. Biofilm was not removed from the sides of the tiles. The biofilm samples were frozen and stored at -20 °C.

Biofilm samples were analyzed for biomass per unit area using ash-free dry mass (AFDM) and then TP content using inductively coupled plasma optical emission spectroscopy (ICP-OES). Biofilm samples were freeze dried at a pressure of 10 to 18 mTorr and a condenser temperature of -60 °C for at least nine days to ensure complete sublimation and constant dry weight. Certified reference materials and process blanks were introduced into each batch. A 100 mL acid-washed media bottle

was labelled and weighed. The freeze-dried sample was then transferred into the media bottle and the weight of the sample transferred recorded. Each media bottle was covered with a ribbed watch glass and samples were dried in the oven at 105 °C for approximately 40 minutes. Media bottles were transferred to a muffle furnace and ashed at 550 °C for three hours, which consisted of one hour for the furnace to come up to temperature and two hours at 550 °C. After the bottles cooled, the bottle and sample were weighed again. The ashed sample mass was determined by subtracting the weight of the media bottle pre-ashing from the weight of the sample and media bottle post-ashing. The AFDM was then determined by subtracting the ashed sample mass from the weight of sample originally transferred.

ICP-OES was used to analyze the TP content of the biofilm samples after processing for AFDM. 10 mL of 1 M HCl was added to each media bottle and the bottles were placed on a shaker table in an incubator for 16 hours at 25 °C to digest. The weight of the HCl added was recorded. A 1:10 analytical dilution was performed on each sample using 2% NO_3. A set of TP standard solutions spread across the analytical range was prepared. An analytical blank was introduced into each ICP batch. Detection limit was 2.17 µg/L and the percent error ranged from 1.6 – 15.0% for the samples at the lowest P concentrations and from 1.9 – 10.0% for samples at the highest P concentrations. The TP of each sampled (mg P) was calculated by multiplying the concentration (mg/L) of P in the sample by the NO_3 dilution factor and by the volume (L) of HCl added (calculated by dividing the weight of HCl added into each sample by 1.063 mg). The TP content of the biofilm, presented as g P, was extrapolated from three tiles (g) to the whole stream using:

$$\text{Equation 4. TP content of biofilm per stream} = \left(\frac{TP\ per\ tile}{A_t} * A_s\right)$$

, where A_t (m^2) = the surface area of three tiles and A_t (m^2) = the wetted surface area of an artificial stream. The TP content of the biofilm as a proportion of the SRP load (%) was calculated by dividing the extrapolated TP content of the biofilm by the cumulative SRP load to each stream, then multiplying by 100, as in Equation 5:

$$\text{Equation 5. TP content of biofilm as proportion of SRP load} = \frac{TP\ biofilm}{SRP\ input} \times 100\%$$

The proportion of the SRP load associated with the pulse contained in the biofilm as TP was calculated using Equation 5, but TP biofilm was calculated by subtracting biofilm TP content in the unenriched from the episodically enriched streams from day 8-11 and SRP input was calculated by

subtracting SRP input to the unenriched from the episodically enriched streams from day 8-11. The TP content per sample was divided by the AFDM per sample (Figure 2.7) to obtain the TP concentration of the biofilm (C_B), presented in mg P/g biofilm. The three samples from each stream were averaged prior to statistical analysis.

Figure 2.6 Scraping biofilm off ceramic tiles into a specimen cup using a toothbrush and mini glass scraper.

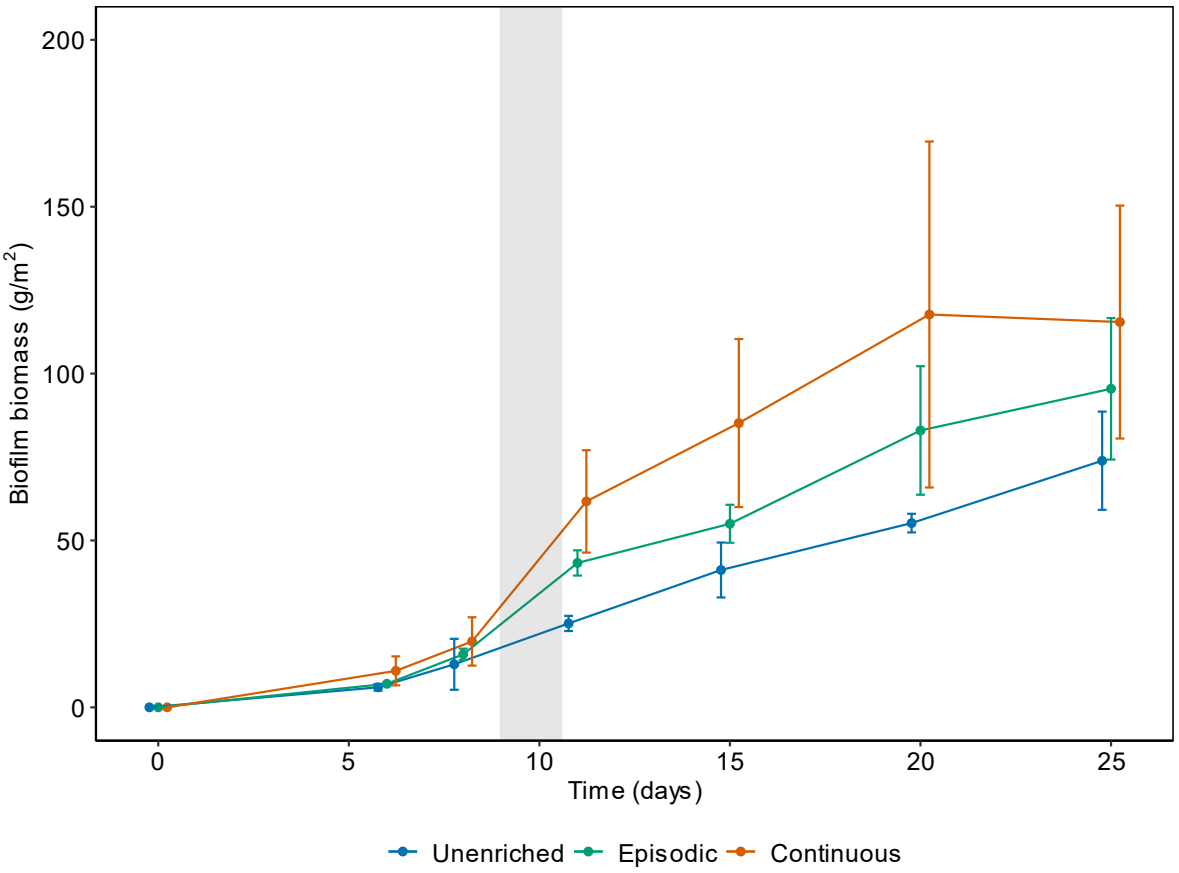

Figure 2.7 Mean biofilm biomass (± one standard deviation) in streams (N = 9) exposed to either unenriched (n = 3), episodically enriched (n = 3), or continuously enriched (n = 3) phosphorus loading patterns. Grey bar indicates duration of the pulse in the episodic loading pattern. A general linear model indicated no differences in biomass among loading patterns at the end of the experiment due to high within-treatment variation (df = 6, F = 2.1, p = 0.20).

2.2.3 TP export

TP concentration of the water at the outflow of each stream was measured to determine TP export. Water samples for TP export were collected approximately every two days throughout the experiment and daily during the pulse, for a total of 14 samples (Table 2.2). For each sampling event, 50 mL of water was collected from the outflow of each stream and preserved using 0.5 mL of 37% H_2SO_4 (Figure 2.5). Water samples were refrigerated at 4 °C prior to being shipped on ice to NLET for TP analysis. TP concentrations were measured using a standard molybdenum blue method via a

colorimeter in a segmented continuous flow analyzer (Environment and Climate Change Canada, 2019, 2020). The detection limit and expected error for TP were 0.5 and 4.9 µg P/L, respectively.

Cumulative TP export was calculated by linearly interpolating TP concentration between measurements, multiplying each concentration by the flow of water out of the stream for each time period, then calculating the cumulative sum. For plotting purposes, cumulative standard deviation was calculated using Equation 2.

2.2.4 Instantaneous SRP uptake

Chamber assays were used to determine instantaneous SRP uptake in all nine streams after six days of growth (day 6), before the pulse (day 8), during the pulse (day 9 and 10), immediately after the pulse (day 11), on days 15 and 20, and on the last day of the experiment (day 25) (Table 2.2). Since the ideal assay time was not established prior to the experiment, we conducted three chamber assays in each stream with differing durations. Plastic chambers were rinsed with water and a randomly selected biofilm-colonized tile was placed in each chamber (Figure 2.8). Each chamber was filled with 164 mL of water from the first reach, lid secured, and start time recorded to the nearest minute. Aliquots of water (45 mL) were collected from the first chamber after approximately one hour, the second chamber after approximately two hours, and the third chamber after approximately three hours. The stop time was recorded to the nearest minute. The water from the second chamber was filtered (sterile cellulose acetate membrane, 0.45 µm) into a 125 mL glass bottle and refrigerated at 4 °C prior to being shipped on ice to NLET for SRP analysis. The first and third water samples were filtered into 45 mL falcon tubes and stored at -20 °C, for use in case the second chamber was depleted of P too quickly or not fast enough. The second chamber was used for most of the sampling events, except for nine samples from day 8 and eight samples from day 9 which came from the first chamber because P concentrations in the second chamber were more than half depleted and sometimes below the limit of detection. No samples from the third chamber were analyzed.

Instantaneous SRP uptake rate (U), presented in g P/m^2/day, was calculated as:

$$\text{Equation 5. } U = \frac{C_0 - C_f}{A * t}$$

, where C_0 (g) is the initial SRP concentration; C_f (g) is the final SRP concentration; A (m^2) is the surface area of one tile; and t is the number of minutes that comprised the assay (Proia et al., 2017).

Figure 2.8 An SRP uptake chamber containing one biofilm-colonized tile and stream water.

Table 2.2 Sampling frequency of each sample type during the 26-day experiment. The 48-hour pulse took place on days 8 – 10.

Sample type	**Days sampled**
N QC	7, 10, 24
SRP QC	1, 10, 24
SRP Export - passive	Continuously from day 0 to 25
SRP Export - discrete	6, 8, 11, 15, 20, 25
Biofilm (TP and biomass)	6, 8, 11, 15, 20, 25
TP Export	2, 4, 6, 8, 9, 10, 11, 13, 15, 16, 19, 20, 23, 25
Instantaneous SRP Uptake	8, 9, 10 11, 15, 20, 25

2.3 Statistical analysis

General linear models (GLMs) were used to test for differences between loading patterns. For each GLM, the fixed factor was loading pattern with three levels (unenriched, episodically enriched, continuously enriched) and significance was assessed using alpha = 0.1. GLMs were conducted on the proportion of SRP not exported on days when DGT passive samplers were replaced in all loading

patterns (day 8 and 25). GLMs were also conducted on the TP content of the biofilm, both as a mass and as a proportion of the SRP load, and on C_B on all sampling days. GLMs were conducted on TP export on the last day of the experiment only. GLMs were also conducted on instantaneous SRP uptake on each sampling day. A cube root transformation was applied to TP content (mass only), C_B, and instantaneous SRP uptake to achieve normality. Tukey's HSD post-hoc tests were conducted on significant GLMs to determine which loading patterns differed and significance was also assessed using alpha = 0.1. GLMs and Tukey's HSD post-hoc tests were performed in R using the glm and emmeans functions, respectively (Lenth et al., 2023; R Core Team, 2021). All means were presented with one standard deviation.

Chapter 3
Results

3.1 Transformation of P by biofilms

Average cumulative SRP export was on average between 59.0 ± 1.0% and 78.3 ± 2.4% less than cumulative SRP input for the duration of the experiment in all loading patterns when measured using DGT passive samplers (Figure 3.1a). Discrete water samples also showed that average cumulative SRP export was less than cumulative SRP input for the duration of the experiment in all loading patterns (Figure 3.2). In the episodically enriched streams, the average proportion of cumulative SRP input not exported as SRP decreased from 73.0 ± 3.6% to 67.5 ± 4.0% (5.5% less) from day 8 to day 10 (the duration of the pulse) in the episodically enriched streams. The amount of SRP exported during the first 24 hours of the pulse was 28.4% less than the amount of SRP exported during the second 24 hours of the pulse in the episodically enriched streams. Average total SRP export associated with the 48-hour pulse (3.25 g) was 1.09 g and thus, 66.5% of the SRP load associated with the pulse was not exported as SRP.

The proportion of the cumulative SRP input not exported as SRP differed between loading patterns before the pulse ($df = 6$, $F = 4.2$, $p = 0.03$), being 10% more in the unenriched than the continuously enriched loading pattern ($p = 0.03$) (Figure 3.1b). However, there was no difference between the episodically enriched and unenriched streams ($p = 0.39$) or between the episodically and continuously enriched streams ($p = 0.29$). At the end of the experiment, the proportion of the cumulative SRP input not exported as SRP differed among loading patterns ($df = 6$, $F = 4.8$, $p = 0.06$), being 18.7% and 19.3% less in the episodically enriched streams than in the unenriched ($p = 0.08$) and continuously enriched streams ($p = 0.08$), respectively. The proportion of the cumulative SRP input not exported as SRP did not differ between the unenriched and continuously enriched streams ($p > 0.99$).

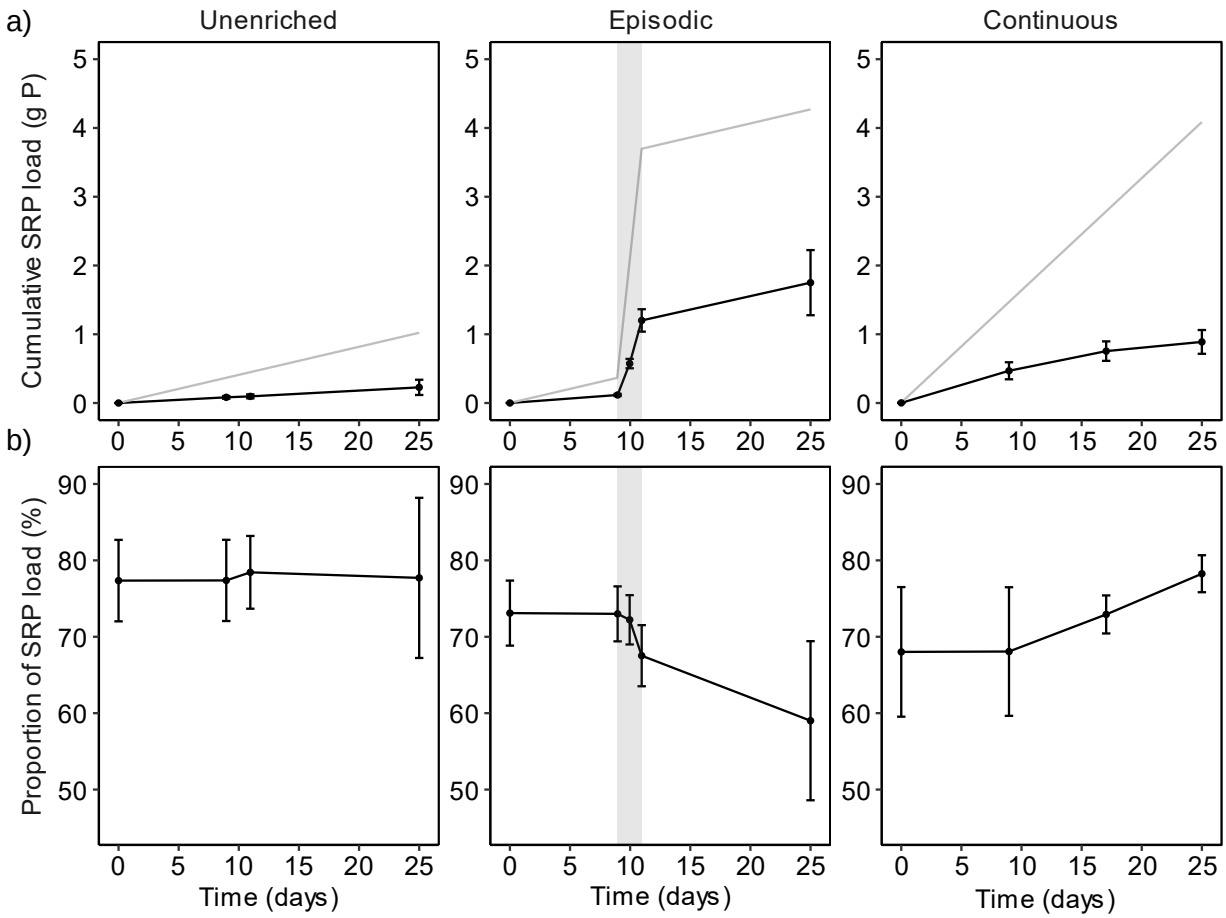

Figure 3.1 Mean cumulative soluble reactive phosphorus (SRP) export (black) (± one cumulative standard deviation) compared to cumulative SRP input (grey) (a) and the mean proportion of the cumulative SRP input not exported as SRP (± one standard deviation) (b) from streams (N = 9) containing biofilms exposed to either unenriched (n = 3) (left), episodically enriched (n = 3) (middle), or continuously enriched (n = 3) (right) phosphorus (P) loading patterns. Grey bar indicates duration of the pulse in the episodic loading pattern.

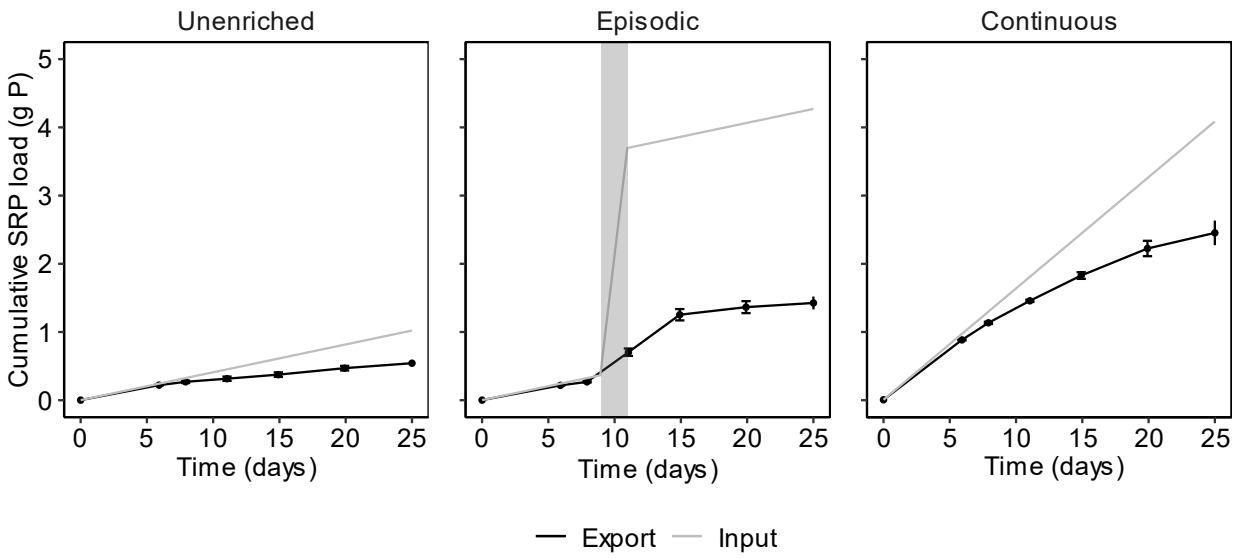

Figure 3.2 Mean cumulative soluble reactive phosphorus (SRP) export (± one cumulative standard deviation) estimated using discrete water samples compared to cumulative SRP input from streams (N = 9) containing biofilms exposed to either unenriched (n = 3) (left), episodically enriched (n = 3) (middle), or continuously enriched (n = 3) (right) phosphorus (P) loading patterns. Grey bar indicates duration of the pulse in the episodic loading pattern. Discrete samples showed that the proportion of the SRP load not exported was 46.9 ± 0.9% in the unenriched, 66.6 ± 0.8% in the episodically enriched, and 40.0 ± 3.4% in the continuously enriched loading pattern.

3.2 Retention of P by biofilms

The average amount of TP in the biofilm increased throughout the experiment in the unenriched streams, reaching an average maximum of 0.19 ± 0.06 g on day 25 (Figure 3.3a). Average TP in the continuously enriched biofilms increased until day 20 then started to decrease, reaching an average maximum of 0.70 ± 0.37 g. The amount of TP in the episodically enriched biofilms increased on average by almost 10-fold from day 8 to day 11 (the duration of the pulse). Biofilms in the episodically enriched streams attained an average maximum concentration of 0.72 ± 0.05 g on day 11. Average TP in the episodically enriched biofilms decreased by 19% between day 11 and day 15 and then another 11% from day 15 to day 25.

Average TP content (i.e., g P) of biofilms in the continuously enriched streams was greater than in the unenriched streams throughout the experiment (Table 3.1; Figure 3.3a). Average biofilm TP

content in the episodically enriched streams did not differ in the amount of mass from the unenriched streams prior to the pulse, but was significantly greater at all sampled time points after the pulse. Episodically and continuously enriched biofilms showed large absolute differences on days 6 through 15 with greater mass switching from the continuously enriched streams prior to the pulse to the episodic streams after the pulse. However, large variation in mass of TP amongst the continuously enriched streams inhibited the detection of statistical differences from the episodically enriched streams on all days but 6 and 11. On day 6, the unenriched and episodically enriched biofilms had approximately half the mass of TP than the continuously enriched streams. The continuously enriched biofilm had approximately double the mass of TP than the unenriched biofilms on day 8, but mass of TP in the episodically enriched did not differ from either the unenriched or continuously enriched biofilms. Mass of TP in biofilms in the episodically enriched streams exceeded the unenriched and continuously enriched biofilms on day 11 by 6- and 1.5-fold, respectively. The mass of TP in the biofilm was on average over 2.5 times higher in the continuously and episodically enriched streams compared to the unenriched streams from day 15 until the end of the experiment.

The amount of TP in the biofilm as a proportion of the SRP load increased overall from day 6 to day 25 in the unenriched and continuously enriched loading patterns, but decreased from day 6 to day 25 in the episodic loading pattern (Figure 3.3b). TP in unenriched biofilms attained an average maximum proportion of the SRP load on day 15 (26.3 ± 5.0%), then decreased by 1.4-fold from day 15 to day 25. Episodically enriched biofilms attained an average maximum proportion of the SRP load as TP on day 8 (24.2 ± 6.0%), then decreased by 2-fold from day 8 to day 25. 18.4% (0.60 g) of the total SRP load delivered during the 48-hour SRP-pulse (3.25 g) was contained in the biofilm as TP. Biofilms attained an average maximum proportion of the SRP load on day 11 in the continuously enriched streams (27.3 ± 5.1), then decreased by 2-fold from day 11 to the end of the experiment. Biofilm TP content was on average 14.4 ± 3.9% (mean of three loading patterns ± one standard deviation) of the SRP load at the end of the experiment, regardless of loading pattern.

The average proportion of the SRP load in biofilms as TP only differed significantly among loading patterns on days 6 and 15 (Table 3.2; Figure 3.3b). Biofilms in the episodically enriched streams contained on average 2.3% more of the SRP load as TP compared to continuously enriched streams on day 6, but did not differ from the unenriched streams. The unenriched biofilms contained a 3.3% and 2.5% higher average proportion of the SRP load as TP on day 15 compared to the episodically and continuously enriched biofilms. The proportion of the SRP load as biofilm TP in the

continuously and episodically enriched biofilms did not differ on day 15. Although the difference was not significant, unenriched biofilms at the end of the experiment contained over 50% more TP on average than enriched biofilms.

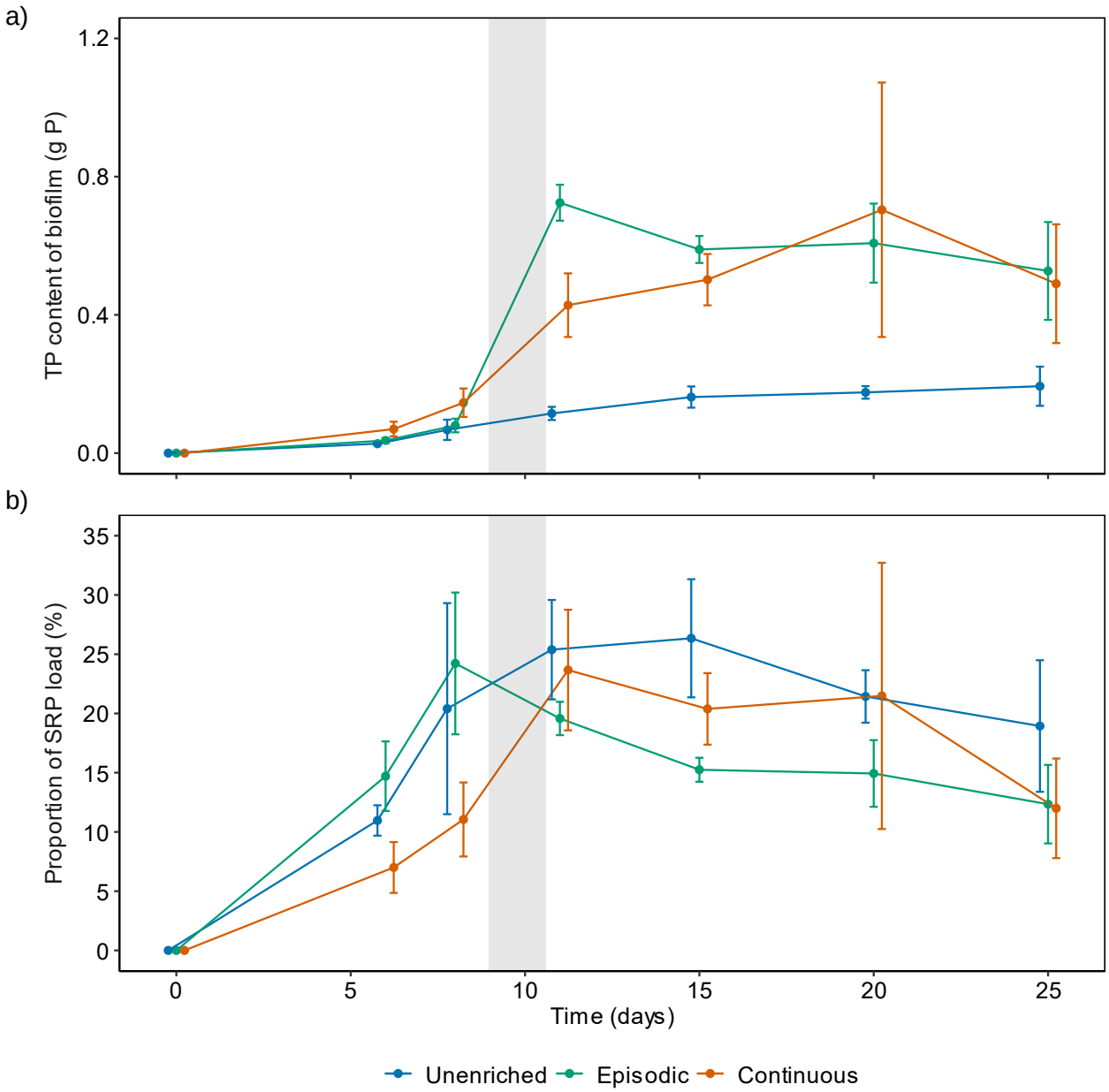

Figure 3.3 Mean total phosphorus (TP) content (± one standard deviation) of stream biofilms (N = 9) extrapolated from a sample composed of three tiles (69.12 cm^2) to the wetted surface area of an artificial stream (3.96 m^2), displayed as an absolute amount (a) and as a proportion of the soluble reactive phosphorus (SRP) load (b). Stream biofilms were exposed to either unenriched (n = 3), episodically enriched (n = 3), or continuously enriched (n = 3) phosphorus (P) loading patterns. Grey bar indicates duration of the pulse in the episodic loading pattern.

Table 3.1 *F* and *p* values from general linear models (GLM) and *p* values from Tukey's HSD post-hoc tests conducted on the average total phosphorus content of stream biofilms on each sampling day for three streams per loading pattern (n = 3, N = 9). GLM degrees of freedom = 6, 2. * indicates a significant *p* value at alpha = 0.1

Time (days)	**GLM**		***p* value from Tukey's HSD**		
	F	***p* value**	**Unenriched - Continuous**	**Unenriched - Episodic**	**Episodic - Continuous**
6	11.5	0.009*	0.008*	0.41	0.04*
8	5.1	0.05*	0.05*	0.74	0.13
11	97.6	< 0.001*	< 0.001*	< 0.001*	0.01*
15	45.4	< 0.001*	0.001*	< 0.001*	0.15
20	14.1	0.005*	0.01*	0.008*	0.97
25	9.6	0.01*	0.03*	0.02*	0.93

Table 3.2 *F* and *p*-values from general linear models (GLM) and p-values from Tukey's HSD post-hoc tests conducted on the total phosphorus content of the biofilm as a proportion of the soluble reactive phosphorus load on each sampling day for three streams per loading pattern (n = 3, N = 9). * indicates a significant *p* value at alpha = 0.1

Time (days)	**GLM**		***p* value from Tukey's HSD**		
	F	***p* value**	**Unenriched -Continuous**	**Unenriched - Episodic**	**Episodic - Continuous**
6	8.4	0.02*	0.17	0.19	0.02*
8	3.3	0.11	-	-	-
11	1.8	0.25	-	-	-
15	7.0	0.03*	0.08*	0.03*	0.64
20	1.5	0.30	-	-	-
25	2.3	0.18	-	-	-

Average cumulative TP export exceeded cumulative SRP input for the entire experiment, except on days 10 through 12 in the unenriched streams, days 11 and 12 in the episodically enriched streams, and days 8 through 14 in the continuously enriched streams (Figure 3.4). Average cumulative TP export during these periods was at maximum 2.2 ± 5.6%, 11.5 ± 0.1%, and 8.5 ± 3.9% lower than cumulative SRP input in the unenriched, episodically enriched, and continuously enriched streams, respectively. Cumulative SRP input was within ± one cumulative standard deviation of cumulative TP export during at least 70% of sampling events. Average cumulative TP export exceeded cumulative SRP input by 0.16 ± 0.10 g (15.2 ± 10.2% of cumulative SRP input) in the unenriched streams, 0.81 ± 0.067 g (19.0 ± 1.6% of cumulative SRP input) in the episodically enriched streams, and 0.46 ± 0.46 g (11.3 ± 11.3% of cumulative SRP input) in the continuously enriched streams by the end of the experiment (day 25). However, a GLM indicated that differences among loading patterns on day 25 were not significant (df = 6, F = 0.6, p = 0.59).

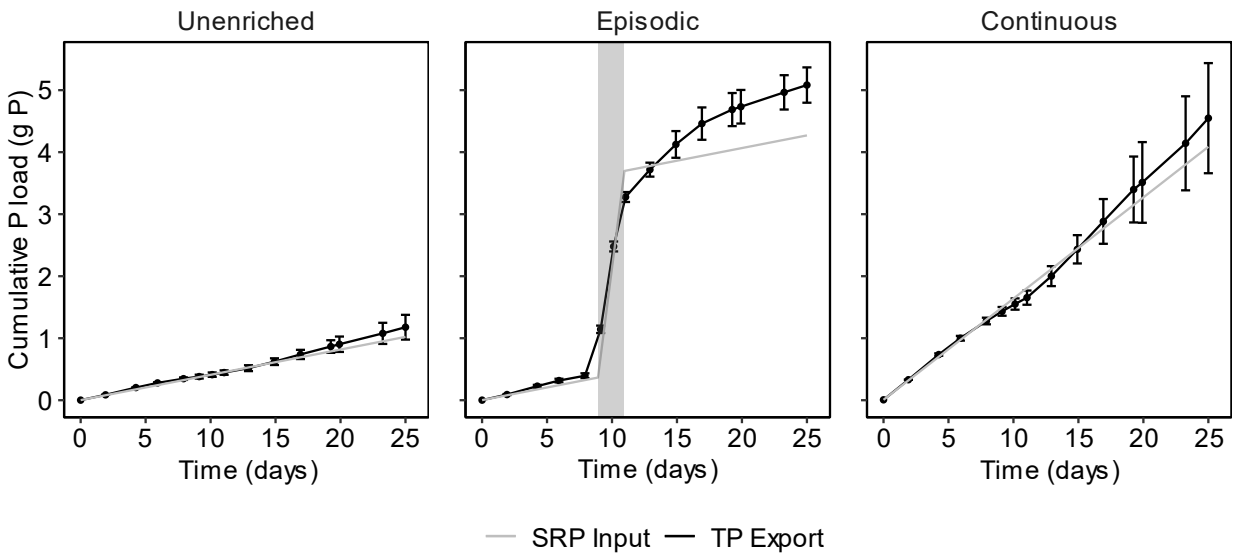

Figure 3.4 Mean cumulative total phosphorus (TP) export (± one cumulative standard deviation) compared to cumulative soluble reactive phosphors (SRP) input from streams (N = 9) containing biofilms exposed to either unenriched (n = 3) (left), episodically enriched (n = 3) (middle), or continuously enriched (n = 3) (right) phosphorus (P) loading patterns. Grey bar indicates duration of the pulse in the episodic loading pattern.

3.3 Biological processes

C_B in all loading patterns was lower at the end of the experiment than on day 6. The unenriched and continuously enriched streams reached an average maximum C_B on day 8 (4.4 ± 0.7 and 6.0 ± 0.9 mg/g, respectively), then decreased on average by approximately 50% from day 8 to day 25 (Figure 3.5). C_B in the episodically enriched streams increased on average by a factor of 3.4 from day 8 to day 11 (after the pulse), attaining an average maximum C_B of 13.2 ± 0.6 mg/g on day 11. C_B in the episodically enriched streams declined on average by 67.2% from day 11 to day 25.

C_B in episodically enriched streams was lower than continuously enriched streams directly before the pulse (day 8), but was higher than in the continuously enriched streams after the pulse until the end of the experiment (day 11-25) (Table 3.3; Figure 3.5). C_B in the continuously enriched biofilms was higher than the unenriched biofilms for the entire experiment, except on day 6 when there were no differences among loading patterns and on day 15 due to high within-treatment variation in the continuously enriched loading pattern. C_B in the episodic loading pattern did not differ from the

unenriched loading pattern on day 8, and both were lower than the continuously enriched biofilms. C_B differed among all three loading patterns on day 11, with the episodic biofilms having the greatest C_B, followed by the continuous (48% lower) and unenriched (63% lower) biofilms. C_B was higher in the episodically enriched biofilms compared to the unenriched or continuously enriched biofilms on day 15 and 20, but continuously enriched biofilms only exceeded the unenriched biofilms on day 15 and did not differ on day 20. C_B differed among all loading patterns at the end of the experiment, being on average over 100% greater in the episodic loading pattern than the unenriched, approximately 20% greater in the episodically than the continuously enriched, and almost 40% greater in the continuously enriched than the unenriched.

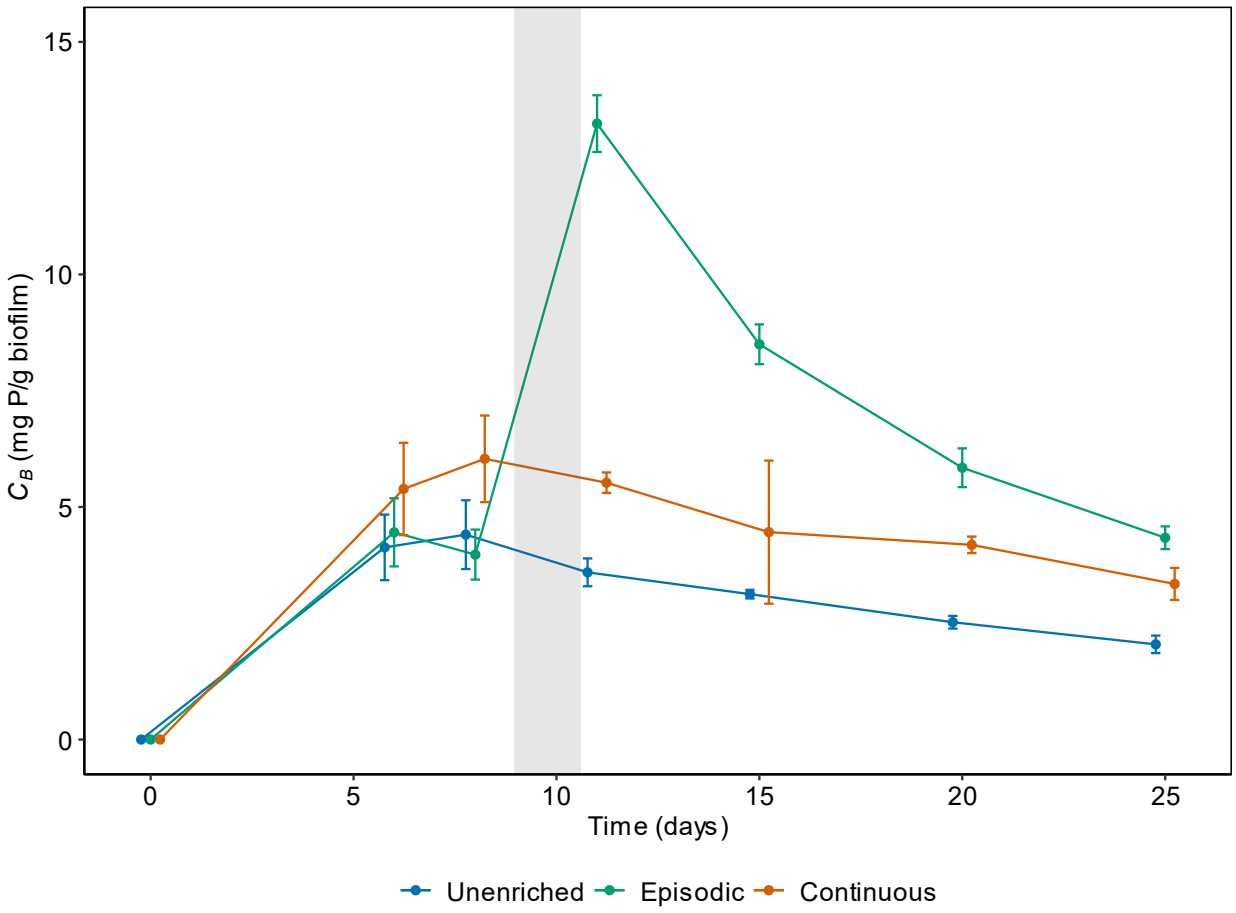

Figure 3.5 Mean total phosphorus concentration of biofilms (C_B) (± one standard deviation) (N = 9) exposed to either unenriched (n = 3), episodically enriched (n = 3), or continuously enriched (n = 3) phosphorus (P) loading patterns. Grey bar indicates duration of the pulse in the episodic loading pattern.

Table 3.3 *F* and *p* values from general linear models (GLM) and *p* values from Tukey's HSD post-hoc tests conducted on C_B on each sampling day for three streams per loading pattern (n = 3, N = 9). GLM degrees of freedom = 6, 2. * indicates a significant *p* value at alpha = 0.1

Time (days)	**GLM**		***p* value from Tukey's HSD**		
	F	***p* value**	**Unenriched - Continuous**	**Unenriched - Episodic**	**Episodic - Continuous**
6	1.9	0.23	-	-	-
8	6.3	0.03*	0.09*	0.73	0.03*
11	453.2	< 0.001*	< 0.001*	< 0.001*	< 0.001*
15	20.0	0.002*	0.25	0.002*	0.01*
20	148.5	<0.001*	< 0.001*	< 0.001*	< 0.001*
25	58.1	<0.001*	0.001*	< 0.001*	0.02*

U in the unenriched streams was frequently below detection limits over the course of the experiment, with *U* not exceeding 0.01 ± 0.006 g/m^2/day (Figure 3.6). *U* in the unenriched streams stayed relatively constant (between below detection and 0.01 ± 0.006 g/m^2/day) throughout the experiment. In contrast, *U* in the continuously enriched streams had an average minimum of 0.05 ± 0.006 g/m^2/day and an average maximum of 0.2 ± 0.03 g/m^2/day and generally decreased on average by approximately 10-fold throughout the experiment, from 0.09 ± 0.0025 g/m^2/day on day 8 to 0.01 ± 0.009 g/m^2/day on day 25. Biofilms in the episodic streams attained an average maximum *U* of 1.3 ± 0.15 g/m^2/day on the first day of the pulse (day 9), then decreased on average by 60% from the first (day 9) to the second day (day 10) of the pulse. *U* in the episodically enriched streams decreased on average a further 55% from day 10 to day 11. *U* in the episodically enriched streams continued to decrease until the end of the experiment, returning to pre-pulse rates on day 25.

U in the continuously enriched streams exceeded the unenriched streams for the entire experiment (except for on day 15 when *U* was equal for all loading patterns) on average by 78 times (Table 3.4; Figure 3.6). Mean *U* by episodically enriched biofilms on day 8 did not differ from unenriched biofilms, but was 36 times lower than continuously enriched biofilms. *U* in the episodically enriched

streams was greater than the continuously and episodically enriched streams from days 9 through 11, exceeding the continuously enriched and unenriched streams by a maximum of 6- and 350-fold over that time, respectively. By the end of the experiment, *U* in the episodically enriched streams returned to a similar rate as that observed in the unenriched streams (difference of 0.003 g/m^2/day), that was 2 times lower than the continuously enriched streams.

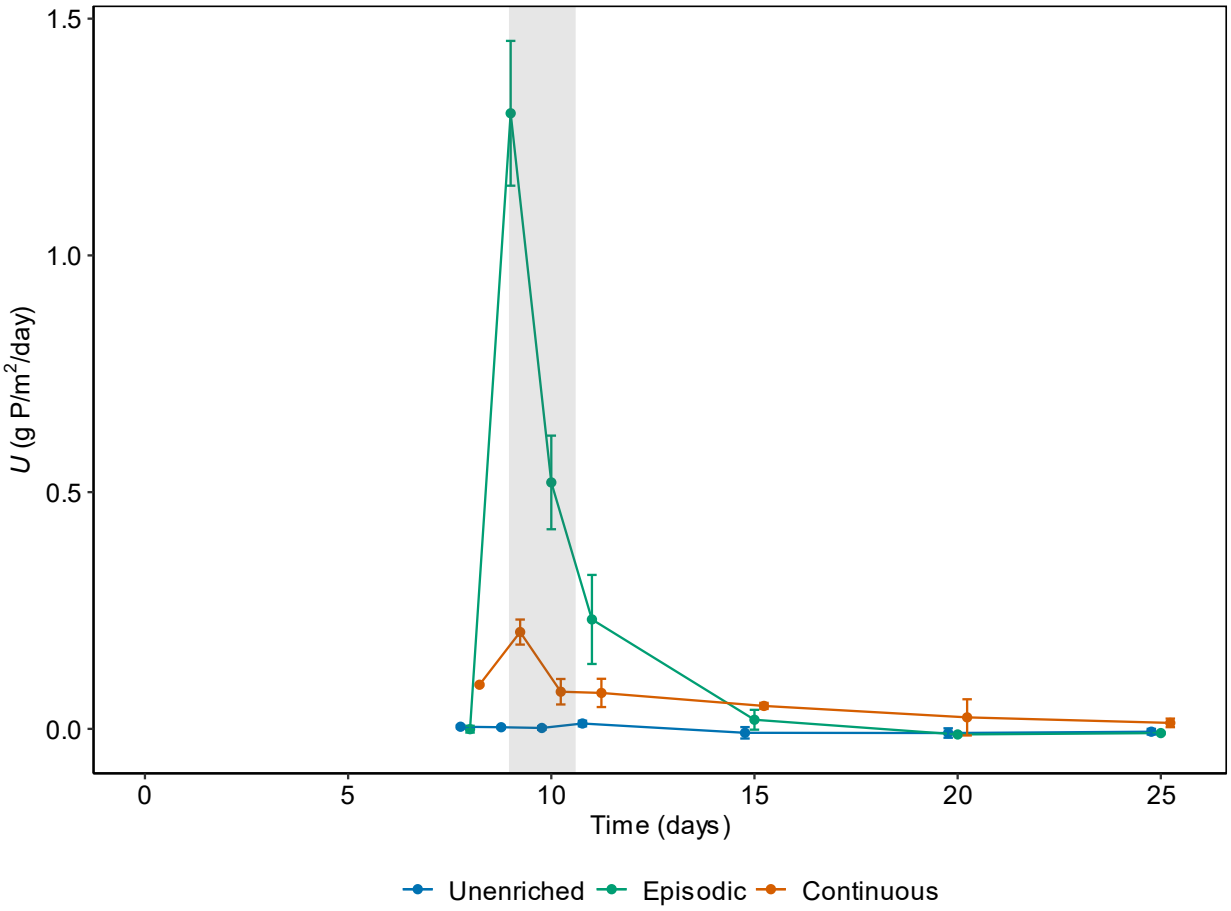

Figure 3.6 Mean instantaneous soluble reactive phosphorus uptake (*U*) (± one standard deviation) by stream biofilms (N = 9) exposed to either unenriched (n = 3), episodically enriched (n = 3), or continuously enriched (n = 3) P loading patterns. Grey bar indicates duration of the pulse in the episodic loading pattern.

Table 3.4 *F* and *p* values from general linear models (GLM) and *p* values from Tukey's HSD post-hoc tests conducted on the *U* on each sampling day for three streams per loading pattern (n = 3, N = 9). GLM degrees of freedom = 6, 2. * indicates a significant *p* value at alpha = 0.1

Time (days)	**GLM**		***p* value from Tukey's HSD**		
	F	***p* value**	**Unenriched - Continuous**	**Unenriched - Episodic**	**Episodic - Continuous**
8	9.4	0.01*	0.05*	0.49	0.01*
9	482.7	< 0.001*	< 0.001*	< 0.001*	< 0.001*
10	37.1	< 0.001*	0.01*	< 0.001*	0.01*
11	25.9	0.001*	0.02*	< 0.001*	0.03*
15	5.3	0.05*	0.04*	0.22	0.44
20	3.7	0.09*	0.15	0.96	0.10
25	22.3	0.002*	0.005*	0.59	0.002*

The colour of the biofilm appeared to differ between unenriched and enriched P treatment levels (Figure 3.7).

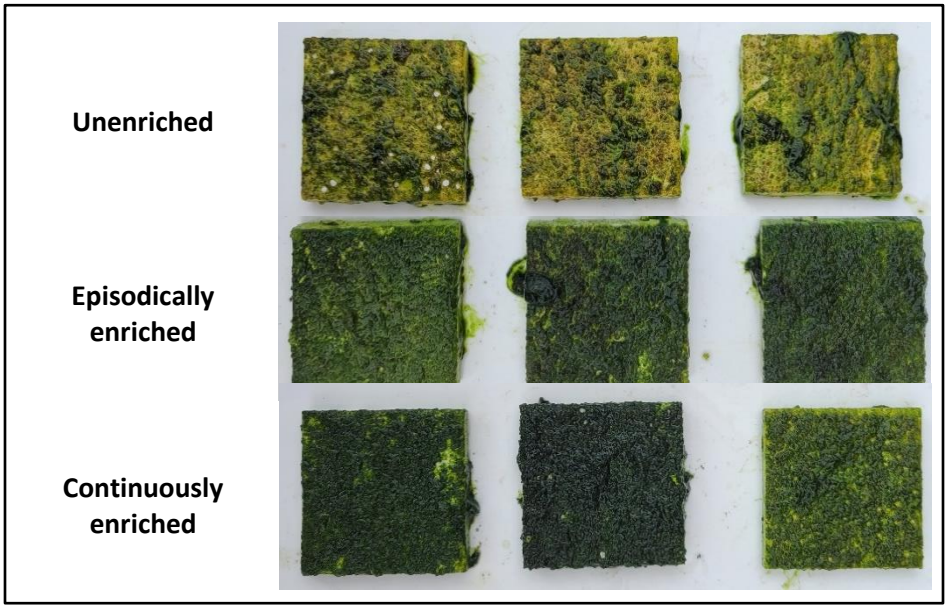

Figure 3.7 Picture of one tile from each stream on the last day of the experiment. The top three tiles were exposed to the unenriched loading pattern, the second row of tiles were exposed to the episodically enriched loading pattern, and the third row of tiles were exposed to the continuously enriched loading pattern.

Chapter 4
Discussion and conclusions

Numerous studies have investigated the response of stream biofilms to P, but few have studied the response under continuous and episodic P delivery patterns, and even less have quantified biofilm P cycling under different loading patterns. This study investigated P cycling by stream biofilms subjected to continuous and episodic SRP loads in artificial streams. It was observed that biofilms retained approximately 15% of SRP under all loading patterns and transformed up to 75% of SRP when it was delivered in a continuous pattern. My findings suggest that stream biofilms acted as P reactors and transitory P sinks.

4.1 Stream biofilms act as P reactors

Biofilms acted as P reactors in conditions emulating low- and mid-order streams during the growing season. Up to three quarters of the SRP load to the artificial streams was not exported as SRP, indicating and affirming previous knowledge that biofilms can transform SRP to other forms of P. Previous research has found that biofilms can transform SRP to particulate and dissolved organic P (Nausch et al., 2018) and unreactive dissolved inorganic P (Pearce et al., 2023), which are typically considered less bioavailable than SRP because these molecules cannot be taken up by biofilm cells without first being cleaved (Reddy et al., 1999). Therefore, transformation of SRP to other forms of P by biofilms has the potential to decrease the bioavailability of P exported to downstream ecosystems.

My findings suggest that the pattern of P delivery to streams impacted the proportion of the SRP load transformed to other forms of P by biofilms. In this experiment, biofilms transformed a larger proportion of the SRP load when SRP was delivered in a continuous compared to an episodic loading pattern, which previous literature suggests is because a continuous loading pattern maximizes the capacity for biological use compared to an episodic loading pattern (Stamm et al., 2014). Indeed, an episodic loading pattern likely reduces the capacity for biological use because a high pulse concentration may surpass the maximum uptake rate of biofilms, leading to a higher proportion of the SRP load bypassing the biofilm than in a continuous loading pattern. Although I observed a sharp increase in biofilm SRP uptake in response to the pulse, only 65% of the pulse was transformed. Thus, the SRP uptake rate was likely not high enough to take up the entire pulse because the SRP uptake rate can be limited by factors such as the amount of biofilm biomass (Sabater et al., 2002),

community composition (Jansson, 1988), and environmental conditions (Balik et al., 2021). However, delivering episodic SRP loads in multiple pulses at a lower concentration instead of a single pulse at a higher concentration may increase the proportion of the SRP load transformed by biofilms. If the pulse concentration is lower, less P may bypass the biofilms and more P transformed since the uptake rate may not be exceeded. Additional studies investigating P forms exported from stream biofilms under various pulse sizes and durations should be conducted to test this hypothesis.

Although approximately one-quarter of the SRP load wasn't transformed, it cannot be precluded that some SRP may have been taken up into the biofilm and released back into the water column as SRP (Zhao et al., 2019). However, it is more likely that most of the SRP exported left the stream before the biofilm could take it up. First, only a small portion of the SRP taken up would likely remain untransformed and have the potential to be released as SRP. Indeed, a previous study showed that over 80% of the SRP taken up into biofilms is transformed to other forms of P within one day (Pearce et al., 2023). Second, internal cycling of P can occur within the biofilm due to the proximity of autotrophic and heterotrophic cells (Scinto & Reddy, 2003), but internal cycling is likely minimal in this experiment since the short experiment duration limited biofilm senescence. Third, P can be released as SRP after transfer from biofilms to grazers (Newbold et al., 1983), but this process is probably limited in these artificial streams due the lack of large grazers. For these reasons, it is likely that most of the SRP exported was not taken up and bypassed the biofilm rather than being released from the biofilm or other trophic levels as SRP.

The approaches used to measure SRP export generated different rates of SRP transformation. Indeed, the discrete approach indicated less transformation of the SRP load in the unenriched and continuously enriched loading patterns and more transformation of the SRP load in the episodically enriched loading pattern than the continuous approach. The results from the DGT passive samplers are likely more accurate because of the low temporal integration of the discrete approach (i.e., six snapshot water samples). Additionally, no discrete water samples were taken during the pulse, leading to not sampling approximately 75% of the SRP load to the episodically enriched streams. In contrast, the DGT samplers were exposed to the stream water continuously throughout the entire experiment, thereby integrating variation in SRP export over time. DGT passive samplers may therefore be useful in field studies when sampling SRP during storm events since it is difficult to predict the occurrence

and duration of storm events and storm events can represent a large part of the annual P load in rural watersheds (Dupas et al., 2015).

4.2 Stream biofilms act as P sinks

Stream biofilms acted as transitory P sinks in an environment representative of headwater and mid-order streams during the growing season. Approximately 15% of the SRP load to each artificial stream was retained in the biofilm at the end of the experiment, thereby delaying export downstream. The storage of P in the biofilm is consistent with previous knowledge that biofilms can play a role in P retention in aquatic ecosystems (Dodds, 2003; Meyer & Likens, 1979; Withers & Jarvie, 2008). Retention of P in biofilms may impact stream P cycling in several ways. First, storage of P in biofilms may increase the amount of time P takes to spiral, since particulate P held in the biofilm is resistance to downstream transport for a period of time (Newbold et al., 1982). Additionally, biomass-associated P can be more easily transferred to higher trophic levels (Meyer & Likens, 1979) and undergo sedimentation (Orihel et al., 2017) than aqueous P, which could temporarily or permanently remove P from the water column. Therefore, retention of P in stream biofilms could delay or prevent P from reaching downstream ecosystems and is likely one of the reasons why P loads entering rivers do not correspond with those measured at the outlet in some mass balance studies (e.g., Svendsen & Kronvang, 1993).

My observations of biofilm P retention showed that biofilms adapted to the pattern of SRP delivery, in that continuously and episodically enriched biofilms retained a similar proportion of the SRP load despite the episodically enriched biofilms having only two days to take up most of the SRP load. Previous studies have indicated that increases in biomass can lead to higher amounts of retention (Dodds, 2003). However, episodically enriched biofilms were still able to retain 18% of the SRP load associated with the pulse despite having 20% less biomass than the continuously enriched biofilms before the pulse. Therefore, the lack of difference in retention cannot be attributed to biomass because there was less biofilm biomass in the episodically than continuously enriched streams before the pulse. And so, biofilms were likely able to retain a similar amount of P under both loading patterns because of uptake kinetics and differences in community composition. The low P concentration before the pulse likely enabled rapid P uptake by episodically enriched biofilms (Price & Carrick, 2016). Additionally, it has been previously demonstrated that biofilm community composition can change with P availability (Lavoie et al., 2008). Since P uptake mechanisms

(Jansson, 1988), P storage capacity (Schade et al., 2011), and optimal ambient P concentration (Ponader et al., 2007) can vary between microorganisms, certain biofilms assemblages could be adapted to taking up and retaining continuous or episodic P loads. However, since this study did not measure community composition, more research would be needed to disentangle the relative contributions of these two processes.

Contrary to my expectations, unenriched and enriched biofilms retained a similar proportion of the SRP load. It was expected that unenriched biofilms would retain a higher proportion of the SRP load than enriched biofilms. Indeed, when stream P concentrations are low, P is typically cycled more efficiently than when P concentrations are high (Covino, 2016) because biota in P-limited streams would maximize P uptake to augment biomass accrual. Unenriched biofilms may have retained the same amount of P as enriched biofilms due to P uptake mechanisms and kinetics. Biofilms may need to take up P actively and therefore expend more energy when in low P environments (Jansson, 1988). Additionally, SRP uptake typically follows a positive linear or Michaelis–Menten model relationship with SRP concentration (Weigelhofer et al., 2018). Thus, uptake and retention by biofilms could likely increase proportionally with P availability.

Stream biofilms provided a transitory P storage zone where the mass of P retained changed over time within loading patterns. For example, the mass of P retained initially increased with biofilm biomass in the continuous loading pattern. However, as the biofilm aged, biomass decreased and led to a decrease in the mass of P retained. The connection between biomass and retention is consistent with previous research, which demonstrated that P initially assimilated into biomass can be released from the biofilm during senescence (Wolfe & Lind, 2010). This relationship between biomass and retention has also been proposed in terrestrial ecosystems, where it is hypothesized that growth-limiting nutrients are conserved during periods of biomass accumulation, but leak out as ecosystem succession progresses and biomass accumulation slows (Vitousek & Reiners, 1975). Therefore, because of the release of P upon senescence, the biofilm is likely only a transitory sink over extended time periods. However, temporal patterns in P retention may differ in real streams where patches of biofilms are at varying stages of succession (Morin & Cattaneo, 1992). Due to the highly heterogenous environment of real streams in comparison to artificial streams, biofilm senescence and release of P may occur at different times among patches within a stream reach. Therefore, field

studies should be conducted to investigate temporal fluxes in biofilm P retention in heterogenous environments.

Patterns in TP export aligned with the mass of TP in the biofilm. TP export was lower than the SRP load when the mass of TP in the biofilm increased the fastest. The TP content of the episodically enriched biofilms increased fastest over the duration of the pulse since high P availability drove uptake, leading to TP export being approximately 10% below the SRP load after the pulse. In the continuously enriched biofilms, TP export was below the SRP load when the increase in the mass of TP was fastest, due to fast biofilm growth. During periods of a slower rate of TP accumulation in the biofilm, error associated with the measurement of TP export masked the effects of biofilm P retention, as anticipated. Since biofilm P content demonstrated that retention was approximately 15% of the SRP load, it is unrealistic that TP export could be 20% higher than the SRP load by the end of the experiment. Using biofilm P content is likely a more accurate method to estimate retention than using TP export because biofilm P content is a direct measurement of retained P.

There are several potential sources of error that could have caused the amount of TP exported to exceed the SRP load. TP inputs not accounted for, such as rain (Migon & Sandroni, 1999), dust (Stoddard et al., 2016), and TP from the initial inoculation could have caused TP export to exceed the SRP load. However, atmospheric deposition of TP in July and August in Southern Ontario is approximately 5 kg/km^2/month (Brown et al., 2011), which would likely equate to on average less than 1% of the P load to the streams. The amount of TP in the 300 mL portions of water-biofilm slurry used to inoculate each stream was likely low due to the small volume. TP export could also have been inflated due to evaporation or pieces of biofilm in the unfiltered water samples, however evaporation would have to be high to cause a detectable change in TP concentration. Therefore, the main cause of the inflated TP export is likely pieces of biofilm in the water samples. This hypothesis is supported by the observation that TP export does not largely surpass SRP load until halfway through the experiment when biofilm biomass is higher and sloughing is more likely. Although TP export was not a reliable measure of retention, since TP export was much larger than SRP export, most of the P exported was not as SRP, confirming a large amount of the SRP was transformed.

4.3 Biofilm response to P

Instantaneous SRP uptake by biofilms responded rapidly to the pulse, demonstrated when biofilm SRP uptake increased from undetectable to 1.3 g P/m^2/day within six hours of the beginning of the pulse. The increase in SRP uptake during the pulse aligns with previous research, which has shown that SRP uptake typically increases with ambient P concentration (Horner et al., 1990; Steinman & Duhamel, 2017). Biofilms exposed to the episodic loading pattern were acclimated to unenriched P concentrations and had low TP content before the pulse. Literature suggests that under these conditions, cells up-regulate phosphate transport proteins (Wurch et al., 2011) and there is a large gradient of low-P inside the biofilm and high-P outside the biofilm (Riegman & Mur, 1984), which likely enabled biofilms to respond rapidly to a P pulse. However, stream biofilms exposed to higher baseline P concentrations may have a limited ability to uptake a P pulse. A previous study determined that biofilms grown in real streams with lower background P concentrations exhibited rapid uptake when supplied with a P addition, while biofilms exposed to higher background P concentrations were not able to uptake a P addition as effectively (Price & Carrick, 2016). The ability of biofilms to transform pulsed P under various baseline P conditions should be further studied because streams can receive both point source loads that increase baseline P concentrations and non-point loads that cause P pulses during periods of high runoff (Withers & Jarvie, 2008).

Patterns of instantaneous SRP uptake by biofilms corroborates differences among loading patterns in the proportion of the SRP load transformed. SRP uptake by episodically enriched biofilms decreased by 60% from the first to the second day of the pulse. Literature suggests that this is likely due to a fading P gradient inside compared to outside the biofilm and an inhibition of the P uptake system in response to intracellular P accumulation (Price & Carrick, 2016). The decrease in SRP uptake from the first day to the second day of the pulse was concurrent with a 30% increase in SRP export. Uptake of SRP into biofilms is one of the first steps in transforming reactive inorganic P to other forms (Price & Carrick, 2016), so it is reasonable to hypothesize that changes in uptake could cause changes in transformation. Since both uptake and transformation decreased on the second day of the pulse, the length of the pulse may alter uptake and the efficiency of SRP transformation.

The TP concentration of the biofilm aligned with loading pattern. The TP concentration of the episodically enriched biofilms increased approximately 3-fold over the duration of the pulse, concurrent to a 10-fold increase in TP content. A recent artificial stream study found a similar

increase in TP content of the biofilm of approximately 3-fold over a 48-h pulse of 400 µg/L after allowing the biofilm to establish for 13 days at 10 µg/L (Pearce et al., 2023). This increase in TP concentration of the biofilm after a P pulse has also been recorded in real streams (Rier et al., 2016). The TP concentration in the episodically enriched biofilms then decreased during the two weeks following the pulse as the TP was assimilated into biofilm biomass, also consistent with a decrease 10 days post-pulse observed in Pearce et al., 2023. TP concentration of the biofilm was consistently higher in the continuously enriched than the unenriched biofilms, likely because there was more P available to the enriched biofilms. Biofilm TP concentration has also been found to increase with SRP enrichment in real streams (Taylor et al., 2022).

4.4 Applications to stream management

My study demonstrated that biofilms transformed a higher proportion of the SRP load when it was delivered in a continuous rather than episodic loading pattern. Since transformation of P by biofilms has the potential to decrease the bioavailability of P exported to downstream ecosystems, maximizing transformation could help further decrease the bioavailability of P in downstream ecosystems. Therefore, P could be released to headwater streams in a continuous loading pattern, when possible, rather than an episodic loading pattern, to maximize transformation by stream biofilms. For example, wastewater lagoons that typically release P-rich effluent in pulses could instead release effluent continuously to reduce SRP losses to downstream ecosystems (Painter et al., 2020). However, my findings also suggested that transformation by biofilms may vary with baseline P concentration, pulse P concentration, and pulse duration. Therefore, careful consideration of these factors is essential to maximize biofilm transformation in streams and reduce the bioavailability of P in downstream ecosystems.

Some watershed models may benefit from applying the knowledge of biofilm P cycling learned in this study. Watershed models that consider forms of P could benefit from incorporating in-stream P cycling by biofilms, since I observed that up to 75% of SRP was transformed by biofilms. However, models that solely focus on TP may not reap the same advantages from incorporating in-stream P cycling by biofilms, since I observed that only approximately 15% of the SRP load was retained in biofilms. The significance of incorporating this information into models may also depend on the time-period addressed, such as event-related loads or annual loads. Biofilm retention was high enough during the pulse that it was reflected in TP export. Therefore, in the case of individual storm events, a

reduction in TP export resulting from the inclusion of biofilm P retention could be meaningful. However, throughout the rest of the experiment, it was observed that biofilm retention was not high enough to be reflected in TP export. Over longer time scales, the impact biofilm P retention may be diminished due to the accumulation of additional error and uncertainty in watershed models.

4.5 Study limitations and future directions

Additional artificial stream studies should be conducted to address research questions that are most immediate based on the scope of my study. I identified that P cycling by biofilms may vary with pulse size, pulse duration, and baseline P concentration, so an additional artificial stream experiment could measure retention and transformation under different pulse sizes, pulse durations, and baseline P concentrations. It was hypothesized that community composition is likely an important factor in biofilm P retention, so an additional artificial stream study should also include a comparison of community composition.

Field studies in real streams should be conducted to validate the findings of P transformation and retention by biofilms in this experiment. An experiment in a real stream could use standardized ceramic tiles as substrate for colonization to reduce variation. Field studies could take advantage of the wide range of environmental conditions present in real streams to investigate how biofilm P cycling may vary spatially. Environmental conditions such grazing pressure from invertebrates (Sabater et al., 2002), different substrate types (Hanrahan et al., 2018), and season (Price & Carrick, 2014) could impact stream P cycling by biofilms but were not investigated in this study.

The artificial streams used in this study emulated shallow streams with high light penetration which are representative of low- and mid-order streams, but P cycling may differ in higher order streams (Ensign & Doyle, 2006) due to conditions such as less light penetration. Future studies should be conducted in conditions that emulate higher order streams to predict how P cycling by biofilms varies across a watershed scale to further inform watershed models. It is also important to investigate P cycling in higher-order streams since P sources such as wastewater treatment plants release effluent to a variety of stream orders (Büttner et al., 2022).

The impact of stream flow on biofilm P cycling is important to explore. During storm events, flow typically increases along with P concentration from non-point sources (Biggs & Close, 1989). Previous research has identified a subsidy-stress relationship between stream velocity and biofilm

biomass (Biggs et al., 1998) and it is suggested that stream flow may impact P cycling in streams. It has been proposed that streams have two modes: a high-discharge throughput mode where P export is high during periods of high flow, and a low-discharge processing mode where P retention is high during periods of low flow (Meyer & Likens, 1979; Withers & Jarvie, 2008). Additional artificial streams studies could be used to measure biofilm P retention and transformation under different flow conditions. By addressing these future directions, we can enhance our understanding of in-stream P cycling.

4.6 Conclusions

Streams are well known to act as active reactors rather than passive pipes (Jarvie et al., 2012), however, the role of biofilms in P retention and transformation under different loading patterns has not previously been isolated and quantified. My findings suggest that biofilms acted as P reactors and transient P sinks in conditions emulating low- and mid-order streams, but transformation by biofilms differed between loading patterns. These findings suggest that loading pattern, as well as pulse duration and pulse and baseline P concentration, should be considered when managing P loads to streams to maximize retention and transformation by biofilms. Biofilm P cycling may be beneficial to include in some watershed models, although its significance may vary depending on the time scale and P species modelled.

Stream biofilms are sometimes regarded as harmful to lotic ecosystems and efforts have been made to curb biofilm growth, since biofilm growth can be excessive under eutrophic conditions (Horner et al., 1990; McDowell et al., 2020). However, stream biofilms were demonstrated to provide an important ecosystem service and could possibly be utilized to reduce eutrophication in downstream ecosystems through transformation of SRP to less bioavailable forms and transient retention of SRP. Additional research in real and artificial streams is required to fill remaining knowledge gaps and determine how biofilm P retention and transformation varies with environmental conditions before this knowledge is applied on a larger scale.

References

Balik, J. A., West, D. C., & Taylor, B. W. (2021). High-discharge disturbance does not alter the seasonal trajectory of nutrient uptake in a montane stream. *Hydrobiologia*, *848*(19), 4535–4550. doi:10.1007/s10750-021-04660-4

Battin, T. J., Kaplan, L. A., Newbold, J. D., & Hansen, C. M. E. (2003). Contributions of microbial biofilms to ecosystem processes in stream mesocosms. *Nature*, *426*(6965), 439–443. doi:10.1038/nature02152

Bayer, M. O., Swartz, L. K., & Lowe, W. H. (2021). Predictors of biofilm biomass in oligotrophic headwater streams. *Northeastern Naturalist*, *28*(1). doi:10.1656/045.028.0103

Beck, W. S., & Hall, E. K. (2018). Confounding factors in algal phosphorus limitation experiments. *PLOS ONE*, *13*(10), e0205684. doi:10.1371/journal.pone.0205684

Bengtsson, M. M., Wagner, K., Schwab, C., Urich, T., & Battin, T. J. (2018). Light availability impacts structure and function of phototrophic stream biofilms across domains and trophic levels. *Molecular Ecology*, *27*(14), 2913–2925. doi:10.1111/mec.14696

Biggs, B. J. F., & Close, M. E. (1989). Periphyton biomass dynamics in gravel bed rivers: The relative effects of flows and nutrients. *Freshwater Biology*, *22*(2), 209–231. doi:10.1111/j.1365-2427.1989.tb01096.x

Biggs, B. J. F., Goring, D. G., & Nikora, V. I. (1998). Subsidy and stress responses of stream periphyton to gradients in water velocity as a function of community growth form. *Journal of Phycology*, *34*(4), 598–607. doi:10.1046/j.1529-8817.1998.340598.x

Borovec, J., Sirová, D., Mošnerová, P., Rejmánková, E., & Vrba, J. (2010). Spatial and temporal changes in phosphorus partitioning within a freshwater cyanobacterial mat community. *Biogeochemistry*, *101*(1/3), 323–333.

Bowes, M. J., Smith, J. T., Jarvie, H. P., & Neal, C. (2008). Modelling of phosphorus inputs to rivers from diffuse and point sources. *Science of The Total Environment*, *395*(2–3), 125–138. doi:10.1016/j.scitotenv.2008.01.054

Brett, M. T., Arhonditsis, G. B., Mueller, S. E., Hartley, D. M., Frodge, J. D., & Funke, D. E. (2005). Non-point-source impacts on stream nutrient concentrations along a forest to urban gradient. *Environmental Management*, *35*(3), 330–342. doi:10.1007/s00267-003-0311-z

Brown, L. J., Taleban, V., Gharabaghi, B., & Weiss, L. (2011). Seasonal and spatial distribution patterns of atmospheric phosphorus deposition to Lake Simcoe, ON. *Journal of Great Lakes Research*, *37*, 15–25. doi:10.1016/j.jglr.2011.01.004

Büttner, O., Jawitz, J. W., Birk, S., & Borchardt, D. (2022). Why wastewater treatment fails to protect stream ecosystems in Europe. *Water Research*, *217*, 118382. doi:10.1016/j.watres.2022.118382

Casas-Ruiz, J. P., Catalán, N., Gómez-Gener, L., von Schiller, D., Obrador, B., Kothawala, D. N., López, P., Sabater, S., & Marcé, R. (2017). A tale of pipes and reactors: Controls on the in-stream dynamics of dissolved organic matter in rivers. *Limnology and Oceanography*, *62*(S1), S85–S94. doi:10.1002/lno.10471

Chambers, P. A., McGoldrick, D. J., Brua, R. B., Vis, C., Culp, J. M., & Benoy, G. A. (2012). Development of environmental thresholds for nitrogen and phosphorus in streams. *Journal of Environmental Quality*, *41*(1), 7–20. doi:10.2134/jeq2010.0273

Chen, D., Hu, M., Wang, J., Guo, Y., & Dahlgren, R. A. (2016). Factors controlling phosphorus export from agricultural/forest and residential systems to rivers in eastern China, 1980–2011. *Journal of Hydrology*, *533*, 53–61. doi:10.1016/j.jhydrol.2015.11.043

Chislock, M. F., Doster, E., Zitomer, R. A., & Wilson, A. E. (2013). *Eutrophication: Causes, Consequences, and Controls in Aquatic Ecosystems*. Nature Education Knowledge. https://www.nature.com/scitable/knowledge/library/eutrophication-causes-consequences-and-controls-in-aquatic-102364466/

Coelho, F., Santos, A., Coimbra, J., Almeida, A., Cunha, A., Cleary, D., Calado, R., & Gomes, N. (2013). Interactive effects of global climate change and pollution on marine microbes: The way ahead. *Ecology and Evolution*, *3*, 1808–1818. doi:10.1002/ece3.565

Correll, D. (1999). Phosphorus: A rate limiting nutrient in surface waters. *Poultry Science*, *78*(5), 674–682. doi:10.1093/ps/78.5.674

Covino, T. (2016). Hydrologic connectivity as a framework for understanding biogeochemical flux through watersheds and along fluvial networks. *Geomorphology*, *277*. doi:10.1016/j.geomorph.2016.09.030

Craggs, R. J., Adey, W. H., Jessup, B. K., & Oswald, W. J. (1996). A controlled stream mesocosm for tertiary treatment of sewage. *Ecological Engineering*, *6*(1–3), 149–169. doi:10.1016/0925-8574(95)00056-9

Davies, J.-M., & Bothwell, M. L. (2012). Responses of lotic periphyton to pulses of phosphorus: P-flux controlled growth rate. *Freshwater Biology*, *57*(12), 2602–2612. doi:10.1111/fwb.12032

Delgado, C., Almeida, S. F. P., Elias, C. L., Ferreira, V., & Canhoto, C. (2017). Response of biofilm growth to experimental warming in a temperate stream. *Ecohydrology*, *10*(6), e1868. doi:10.1002/eco.1868

DeNicola, D. M., McNair, J. N., & Suh, J. (2021). A stochastic model of epilithic algal succession and patch dynamics in streams. *Ecosphere*, *12*(7), e03566. doi:10.1002/ecs2.3566

DGT Research. (2023a). *DGT device for phosphate using a ferrihydrite binding layer*. https://www.dgtresearch.com/detailed-user-guides/Phosphate-FeO-detailed-guide-A2-2020.pdf

DGT Research. (2023b). *Diffusion Coefficients*. https://www.dgtresearch.com/diffusion-coefficients/

Dieter, D., Herzog, C., & Hupfer, M. (2015). Effects of drying on phosphorus uptake in re-flooded lake sediments. *Environmental Science and Pollution Research*, *22*(21), 17065–17081. doi:10.1007/s11356-015-4904-x

Ding, X., Shen, Z., Hong, Q., Yang, Z., Wu, X., & Liu, R. (2010). Development and test of the Export Coefficient Model in the Upper Reach of the Yangtze River. *Journal of Hydrology*, *383*(3), 233–244. doi:10.1016/j.jhydrol.2009.12.039

Dodds, W. K. (2003). The role of periphyton in phosphorus retention in shallow freshwater aquatic systems. *Journal of Phycology*, *39*(5), 840–849. doi:10.1046/j.1529-8817.2003.02081.x

Dorioz, J. M., Pilleboue, E., & Ferhi, A. (1989). Phosphorus dynamics in watersheds: Role of trapping processes in sediments. *Water Research*, *23*(2), 147–158. doi:10.1016/0043-1354(89)90038-9

Drolc, A., & Zagorc Koncan, J. (2002). Estimation of sources of total phosphorus in a river basin and assessment of alternatives for river pollution reduction. *Environment International*, *28*(5), 393–400. doi:10.1016/S0160-4120(02)00062-4

Dupas, R., Tavenard, R., Fovet, O., Gilliet, N., Grimaldi, C., & Gascuel-Odoux, C. (2015). Identifying seasonal patterns of phosphorus storm dynamics with dynamic time warping. *Water Resources Research*, *51*(11), 8868–8882. doi:10.1002/2015WR017338

Ensign, S. H., & Doyle, M. W. (2006). Nutrient spiraling in streams and river networks. *Journal of Geophysical Research: Biogeosciences*, *111*(G4). doi:10.1029/2005JG000114

Environment and Climate Change Canada. (2019). *Standard operating procedure for the analysis of orthophosphate (SRP) in waters by automated continuous flow analyzer colorimetric ascorbic acid method.*

Environment and Climate Change Canada. (2020). *Standard operating procedure for the analysis of total phosphorus in waters by automated continuous flow analyzer colorimetric ascorbic acid method*.

Environment and Climate Change Canada. (2018, December 15). *National Laboratory for Environmental Testing*. https://profils-profiles.science.gc.ca/en/research-centre/national-laboratory-environmental-testing

Feijoó, C., Giorgi, A., & Ferreiro, N. (2011). Phosphate uptake in a macrophyte-rich Pampean stream. *Limnologica*, *41*(4), 285–289. doi:10.1016/j.limno.2010.11.002

Filazzola, A., & Cahill Jr, J. F. (2021). Replication in field ecology: Identifying challenges and proposing solutions. *Methods in Ecology and Evolution*, *12*(10), 1780–1792. doi:10.1111/2041-210X.13657

Findlay, D. L., & Kasian, S. E. M. (1987). Phytoplankton community responses to nutrient addition in Lake 226, Experimental Lakes Area, Northwestern Ontario. *Canadian Journal of Fisheries and Aquatic Sciences*, *44*(S1), s35–s46. doi:10.1139/f87-278

Gardner, L. R. (1990). The role of rock weathering in the phosphorus budget of terrestrial watersheds. *Biogeochemistry*, *11*(2), 97–110.

Gautam, A., Lear, G., & Lewis, G. D. (2022). Time after time: Detecting annual patterns in stream bacterial biofilm communities. *Environmental Microbiology*, *24*(5), 2502–2515. doi:10.1111/1462-2920.16017

Gelwick, F. P., & McIntyre, P. B. (2017). *Methods in Stream Ecology—Chapter 22: Trophic Relations of Stream Fishes* (3rd ed., Vol. 1). Elsevier Inc. doi:10.1016/B978-0-12-416558-8.00022-6

Graba, M., Kettab, A., Sauvage, S., & Sanchez-Pérez, J. M. (2012). On modeling chronic detachment of periphyton in artificial rough, open channel flow. *Desalination and Water Treatment*, *41*(1–3), 79–87. doi:10.1080/19443994.2012.664681

Hach Canada. (2023a). *DR 1900 Portable Spectrophotometer*. https://ca.hach.com/spectrophotometers/dr-1900-portable-spectrophotometer/family?productCategoryId=22219119481

Hach Canada. (2023b). *Nitrate TNTplus Vial Test*. https://www.hach.com/p-nitrate-tntplus-vial-tests/TNT835

Haggard, B., & Sharpley, A. (2006). *Phosphorus Transport in Streams* (pp. 105–130). doi:10.1201/9781420005417.ch5

Hanrahan, B. R., Tank, J. L., Aubeneau, A. F., & Bolster, D. (2018). Substrate-specific biofilms control nutrient uptake in experimental streams. *Freshwater Science*, *37*(3), 456–471. doi:10.1086/699004

Horner, R. R., Welch, E. B., Seeley, M. R., & Jacoby, J. M. (1990). Responses of periphyton to changes in current velocity, suspended sediment and phosphorus concentration. *Freshwater Biology*, *24*(2), 215–232. doi:10.1111/j.1365-2427.1990.tb00704.x

House, W. A. (2003). Geochemical cycling of phosphorus in rivers. *Applied Geochemistry*, *18*(5), 739–748. doi:10.1016/S0883-2927(02)00158-0

Humphrey, K. P., & Stevenson, R. J. (1992). Responses of benthic algae to pulses in current and nutrients during simulations of subscouring spates. *Journal of the North American Benthological Society*, *11*(1), 37–48. doi:10.2307/1467880

Jansson, M. (1988). Phosphate uptake and utilization by bacteria and algae. *Hydrobiologia*, *170*(1), 177–189. doi:10.1007/BF00024904

Jarvie, H. P., Jürgens, M. D., Williams, R. J., Neal, C., Davies, J. J. L., Barrett, C., & White, J. (2005). Role of river bed sediments as sources and sinks of phosphorus across two major eutrophic UK river basins: The Hampshire Avon and Herefordshire Wye. *Journal of Hydrology*, *304*(1), 51–74. doi:10.1016/j.jhydrol.2004.10.002

Jarvie, H. P., Neal, C., Warwick, A., White, J., Neal, M., Wickham, H. D., Hill, L. K., & Andrews, M. C. (2002). Phosphorus uptake into algal biofilms in a lowland chalk river. *The Science of the Total Environment*, *282–283*, 353–373. doi:10.1016/s0048-9697(01)00924-x

Jarvie, H. P., Sharpley, A. N., Scott, J. T., Haggard, B. E., Bowes, M. J., & Massey, L. B. (2012). Within-river phosphorus retention: Accounting for a missing piece in the watershed phosphorus puzzle. *Environmental Science & Technology*, *46*(24), 13284–13292. doi:10.1021/es303562y

Jenny, J.-P., Anneville, O., Arnaud, F., Baulaz, Y., Bouffard, D., Domaizon, I., Bocaniov, S. A., Chèvre, N., Dittrich, M., Dorioz, J.-M., Dunlop, E. S., Dur, G., Guillard, J., Guinaldo, T., Jacquet, S., Jamoneau, A., Jawed, Z., Jeppesen, E., Krantzberg, G., … Weyhenmeyer, G. A.

(2020). Scientists' warning to humanity: Rapid degradation of the world's large lakes. *Journal of Great Lakes Research*, *46*(4), 686–702. doi:10.1016/j.jglr.2020.05.006

Jessup, C. M., Kassen, R., Forde, S. E., Kerr, B., Buckling, A., Rainey, P. B., & Bohannan, B. J. M. (2004). Big questions, small worlds: Microbial model systems in ecology. *Trends in Ecology & Evolution*, *19*(4), 189–197. doi:10.1016/j.tree.2004.01.008

Lavoie, I., Campeau, S., Darchambeau, F., Cabana, G., & Dillon, P. J. (2008). Are diatoms good integrators of temporal variability in stream water quality? *Freshwater Biology*, *53*(4), 827–841. doi:10.1111/j.1365-2427.2007.01935.x

Lenth, R. V., Bolker, B., Buerkner, P., Giné-Vázquez, I., Herve, M., Jung, M., Love, J., Miguez, F., Riebl, H., & Singmann, H. (2023). *emmeans: Estimated Marginal Means, aka Least-Squares Means* (1.8.6) [Computer software]. https://cran.r-project.org/web/packages/emmeans/index.html

Lindberg, V. (2000, July 1). *Uncertainties and Error Propagation* [Louisiana State University]. https://www.geol.lsu.edu/jlorenzo/geophysics/uncertainties/Uncertaintiespart2.html

Lock, M. A., Wallace, R. R., Costerton, J. W., Ventullo, R. M., & Charlton, S. E. (1984). River epilithon: Toward a structural-functional model. *Oikos*, *42*(1), 10–22. doi:10.2307/3544604

Lottig, N. R., & Stanley, E. H. (2007). Benthic sediment influence on dissolved phosphorus concentrations in a headwater stream. *Biogeochemistry*, *84*(3), 297–309.

Lu, H., Wan, J., Li, J., Shao, H., & Wu, Y. (2016). Periphytic biofilm: A buffer for phosphorus precipitation and release between sediments and water. *Chemosphere*, *144*, 2058–2064. doi:10.1016/j.chemosphere.2015.10.129

Mainstone, C. P., & Parr, W. (2002). Phosphorus in rivers—Ecology and management. *Science of The Total Environment*, *282–283*, 25–47. doi:10.1016/S0048-9697(01)00937-8

Mason, S., Hamon, R., Nolan, A., Zhang, H., & Davison, W. (2005). Performance of a mixed binding layer for measuring anions and cations in a single assay using the Diffusive Gradients in Thin Films technique. *Analytical Chemistry*, *77*(19), 6339–6346. doi:10.1021/ac0507183

Matheson, F., Tank, J., & Costley, K. (2011). Land use influences stream nitrate uptake in the Lake Taupo catchment. *New Zealand Journal of Marine and Freshwater Research*, *45*(2), 287–300. doi:10.1080/00288330.2011.562143

McDowell, R. W., Noble, A., Pletnyakov, P., Haggard, B. E., & Mosley, L. M. (2020). Global mapping of freshwater nutrient enrichment and periphyton growth potential. *Scientific Reports*, *10*(1), Article 1. doi:10.1038/s41598-020-60279-w

McIntyre, P. B., Flecker, A. S., Vanni, M. J., Hood, J. M., Taylor, B. W., & Thomas, S. A. (2008). Fish distributions and nutrient cycling in streams: Can fish create biogeochemical hotspots? *Ecology*, *89*(8), 2335–2346. doi:10.1890/07-1552.1

Meyer, J. L., & Likens, G. E. (1979). Transport and transformation of phosphorus in a forest stream ecosystem. *Ecology*, *60*(6), 1255–1269. doi:10.2307/1936971

Migon, C., & Sandroni, V. (1999). Phosphorus in rainwater: Partitioning inputs and impact on the surface coastal ocean. *Limnology and Oceanography*, *44*(4), 1160–1165. doi:10.4319/lo.1999.44.4.1160

Morin, A., & Cattaneo, A. (1992). Factors affecting sampling variability of freshwater periphyton and the power of periphyton studies. *Canadian Journal of Fisheries and Aquatic Sciences*, *49*(8), 1695–1703. doi:10.1139/f92-188

Mulholland, P. J., Newbold, J. D., Elwood, J. W., & Hom, C. L. (1983). The effect of grazing intensity on phosphorus spiralling in autotropic streams. *Oecologia*, *58*(3), 358–366. doi:10.1007/BF00385236

Nausch, M., Achterberg, E. P., Bach, L. T., Brussaard, C. P. D., Crawfurd, K. J., Fabian, J., Riebesell, U., Stuhr, A., Unger, J., & Wannicke, N. (2018). Concentrations and uptake of dissolved organic phosphorus compounds in the baltic sea. *Frontiers in Marine Science*, *5*. https://www.frontiersin.org/articles/10.3389/fmars.2018.00386

Neal, C. (2001). The potential for phosphorus pollution remediation by calcite precipitation in UK freshwaters. *Hydrology and Earth System Sciences*, *5*(1), 119–131. doi:10.5194/hess-5-119-2001

Newbold, J. D., Elwood, J. W., O'Neill, R. V., & Sheldon, A. L. (1983). Phosphorus dynamics in a woodland stream ecosystem: A study of nutrient spiralling. *Ecology*, *64*(5), 1249–1265. doi:10.2307/1937833

Newbold, J. D., O'Neill, R. V., Elwood, J. W., & Van Winkle, W. (1982). Nutrient spiralling in streams: Implications for nutrient limitation and invertebrate activity. *The American Naturalist*, *120*(5), 628–652.

Onset's HOBO. (2023). *HOBO Pendant Temperature/Light 64K Data Logger*. https://www.onsetcomp.com/products/data-loggers/ua-002-64

Orihel, D. M., Baulch, H. M., Casson, N. J., North, R. L., Parsons, C. T., Seckar, D. C. M., & Venkiteswaran, J. J. (2017). Internal phosphorus loading in Canadian fresh waters: A critical review and data analysis. *Canadian Journal of Fisheries and Aquatic Sciences*, *74*(12), 2005–2029. doi:10.1139/cjfas-2016-0500

OTT Hydromet. (2019). *Water Flow Meter*. https://www.ott.com/products/water-flow-3/ott-mf-pro-water-flow-meter-968/

Painter, K. J., Brua, R. B., Spoelstra, J., Koehler, G., & Yates, A. G. (2020). Fate of bioavailable nutrients released to a stream during episodic effluent releases from a municipal wastewater treatment lagoon. *Environmental Science: Processes & Impacts*, *22*(12), 2374–2387. doi:10.1039/D0EM00315H

Parker, S. P., Bowden, W. B., Flinn, M. B., Giles, C. D., Arndt, K. A., Beneš, J. P., & Jent, D. G. (2018). Effect of particle size and heterogeneity on sediment biofilm metabolism and nutrient uptake scaled using two approaches. *Ecosphere*, *9*(3), e02137. doi:10.1002/ecs2.2137

Pearce, N. J. T., Parsons, C. T., Pomfret, S. M., & Yates, A. G. (2023). Periphyton phosphorus uptake in response to dynamic concentrations in streams: Assimilation and changes to intracellular speciation. *Environmental Science & Technology*, *57*(11), 4643–4655. doi:10.1021/acs.est.2c06285

Pearce, N. J. T., Thomas, K. E., Lavoie, I., Chambers, P. A., & Yates, A. G. (2020). Episodic loadings of phosphorus influence growth and composition of benthic algae communities in artificial stream mesocosms. *Water Research*, *185*, 116139. doi:10.1016/j.watres.2020.116139

Ponader, K. C., Charles, D. F., & Belton, T. J. (2007). Diatom-based TP and TN inference models and indices for monitoring nutrient enrichment of New Jersey streams. *Ecological Indicators*, *7*(1), 79–93. doi:10.1016/j.ecolind.2005.10.003

Price, K. J., & Carrick, H. J. (2013). Effects of physical disturbance on phosphorus uptake in temperate stream biofilms. *Inland Waters*, *3*(3), 321–330. doi:10.5268/IW-3.3.551

Price, K. J., & Carrick, H. J. (2014). Quantitative evaluation of spatiotemporal phosphorus fluxes in stream biofilms. *Freshwater Science*, *33*(1), 99–111. doi:10.1086/674874

Price, K. J., & Carrick, H. J. (2016). Effects of experimental nutrient loading on phosphorus uptake by biofilms: Evidence for nutrient saturation in mid-Atlantic streams. *Freshwater Science*, *35*(2), 503–517. doi:10.1086/686269

Proia, L., Romaní, A., & Sabater, S. (2017). Biofilm phosphorus uptake capacity as a tool for the assessment of pollutant effects in river ecosystems. *Ecotoxicology*, *26*(2), 271–282. doi:10.1007/s10646-017-1761-z

R Core Team. (2021). *R: A language and environment for statistical computing. R Foundation for Statistical Computing* (4.1) [Computer software]. https://www.R-project.org/

Raney, S. M., & Eimers, M. C. (2014). Unexpected declines in stream phosphorus concentrations across southern Ontario. *Canadian Journal of Fisheries and Aquatic Sciences*, *71*(3), 337–342. doi:10.1139/cjfas-2013-0300

Reddy, K. R., Kadlec, R. H., Flaig, E., & Gale, P. M. (1999). Phosphorus retention in streams and vetlands: A review. *Critical Reviews in Environmental Science and Technology*, *29*(1), 83–146. doi:10.1080/10643389991259182

Ren, Z., Niu, D., Ma, P., Wang, Y., Wang, Z., Fu, H., & Elser, J. J. (2020). Bacterial communities in stream biofilms in a degrading grassland watershed on the Qinghai–Tibet Plateau. *Frontiers in Microbiology*, *11*. https://www.frontiersin.org/articles/10.3389/fmicb.2020.01021

Richards, S., Paterson, E., Withers, P. J. A., & Stutter, M. (2016). Septic tank discharges as multi-pollutant hotspots in catchments. *Science of The Total Environment*, *542*, 854–863. doi:10.1016/j.scitotenv.2015.10.160

Riegman, R., & Mur, L. R. (1984). Regulation of phosphate uptake kinetics in Oscillatoria agardhii. *Archives of Microbiology*, *139*(1), 28–32. doi:10.1007/BF00692707

Rier, S. T., Kinek, K. C., Hay, S. E., & Francoeur, S. N. (2016). Polyphosphate plays a vital role in the phosphorus dynamics of stream periphyton. *Freshwater Science*, *35*(2), 490–502. doi:10.1086/685859

Sabater, S., Guasch, H., Romaní, A., & Muñoz, I. (2002). The effect of biological factors on the efficiency of river biofilms in improving water quality. *Hydrobiologia*, *469*(1), 149–156. doi:10.1023/A:1015549404082

Sagarin, R. D., Adams, J., Blanchette, C. A., Brusca, R. C., Chorover, J., Cole, J. E., Micheli, F., Munguia-Vega, A., Rochman, C. M., Bonine, K., van Haren, J., & Troch, P. A. (2016).

Between control and complexity: Opportunities and challenges for marine mesocosms. *Frontiers in Ecology and the Environment*, *14*(7), 389–396.

Schade, J. D., MacNEILL, K., Thomas, S. A., CAMILLE McNEELY, F., Welter, J. R., Hood, J., Goodrich, M., Power, M. E., & Finlay, J. C. (2011). The stoichiometry of nitrogen and phosphorus spiralling in heterotrophic and autotrophic streams. *Freshwater Biology*, *56*(3), 424–436. doi:10.1111/j.1365-2427.2010.02509.x

Schiller, D. V., Martí, E., Riera, J. L., & Sabater, F. (2007). Effects of nutrients and light on periphyton biomass and nitrogen uptake in Mediterranean streams with contrasting land uses. *Freshwater Biology*, *52*(5), 891–906. doi:10.1111/j.1365-2427.2007.01742.x

Scinto, L. J., & Reddy, K. R. (2003). Biotic and abiotic uptake of phosphorus by periphyton in a subtropical freshwater wetland. *Aquatic Botany*, *77*(3), 203–222. doi:10.1016/S0304-3770(03)00106-2

Shen, J., Yuan, L., Zhang, J., Li, H., Bai, Z., Chen, X., Zhang, W., & Zhang, F. (2011). Phosphorus dynamics: From soil to plant. *Plant Physiology*, *156*(3), 997–1005. doi:10.1104/pp.111.175232

Smith, V. H. (2003). Eutrophication of freshwater and coastal marine ecosystems a global problem. *Environmental Science and Pollution Research*, *10*(2), 126–139. doi:10.1065/espr2002.12.142

Sonoda, K., Yeakley, J. Alan., & Walker, C. E. (2001). Near-stream landuse effects on streamwater nutrient distribution in an urbanizing watershed. *JAWRA Journal of the American Water Resources Association*, *37*(6), 1517–1532. doi:10.1111/j.1752-1688.2001.tb03657.x

Stamm, C., Jarvie, H. P., & Scott, T. (2014). What's more important for managing phosphorus: Loads, concentrations or both? *Environmental Science & Technology*, *48*(1), 23–24. doi:10.1021/es405148c

Steinman, A. D., & Duhamel, S. (2017). *Methods in Stream Ecology—Chapter 33: Phosphorus Limitation, Uptake, and Turnover in Benthic Stream Algae* (3rd ed., Vol. 1). Elsevier Inc. doi:10.1016/B978-0-12-416558-8.00022-6

Stoddard, J. L., Van Sickle, J., Herlihy, A. T., Brahney, J., Paulsen, S., Peck, D. V., Mitchell, R., & Pollard, A. I. (2016). Continental-scale increase in lake and stream phosphorus: Are oligotrophic systems disappearing in the United States? *Environmental Science & Technology*, *50*(7), 3409–3415. doi:10.1021/acs.est.5b05950

Stutter, M. I., Demars, B. O. L., & Langan, S. J. (2010). River phosphorus cycling: Separating biotic and abiotic uptake during short-term changes in sewage effluent loading. *Water Research*, *44*(15), 4425–4436. doi:10.1016/j.watres.2010.06.014

Suberkropp, K., & Chauvet, E. (1995). Regulation of leaf breakdown by fungi in streams: Influences of water chemistry. *Ecology*, *76*(5), 1433–1445. doi:10.2307/1938146

Svendsen, L. M., & Kronvang, B. (1993). Retention of nitrogen and phosphorus in a Danish lowland river system: Implications for the export from the watershed. *Hydrobiologia*, *251*(1), 123–135. doi:10.1007/BF00007172

Taylor, S., Saia, S. M., Buda, A. R., Regan, J. M., Walter, M. T., & Carrick, H. J. (2022). Polyphosphate accumulation tracks incremental P-enrichment in a temperate watershed (Pennsylvania, United States) as an indicator of stream ecosystem legacy P. *Frontiers in Environmental Science*, *10*. https://www.frontiersin.org/articles/10.3389/fenvs.2022.920733

Tiessen, H., Lopez-Hernandez, D., & Salcedo, I. H. (1989). *Phosphorus cycles in terrestrial and aquatic ecosystems; Regional workshop 3: South and Central America*. 264. https://andrewsforest.oregonstate.edu/sites/default/files/lter/pubs/pdf/pub1303.pdf

Vitousek, P., & Reiners, W. (1975). Ecosystem succession and nutrient retention: A hypothesis. *Bioscience*, *25*, 376–381. doi:10.2307/1297148

Vymazal, J. (1988). The use of periphyton communities for nutrient removal from polluted streams. *Hydrobiologia*, *166*(3), 225–237. doi:10.1007/BF00008132

Weigelhofer, G., Ramião, J. P., Puritscher, A., & Hein, T. (2018). How do chronic nutrient loading and the duration of nutrient pulses affect nutrient uptake in headwater streams? *Biogeochemistry*, *141*(2), 249–263. doi:10.1007/s10533-018-0518-y

Williams, M. R., Livingston, S. J., Penn, C. J., Smith, D. R., King, K. W., & Huang, C. (2018). Controls of event-based nutrient transport within nested headwater agricultural watersheds of the western Lake Erie basin. *Journal of Hydrology*, *559*, 749–761. doi:10.1016/j.jhydrol.2018.02.079

Williamson, T. J., Cross, W. F., Benstead, J. P., Gíslason, G. M., Hood, J. M., Huryn, A. D., Johnson, P. W., & Welter, J. R. (2016). Warming alters coupled carbon and nutrient cycles in experimental streams. *Global Change Biology*, *22*(6), 2152–2164. doi:10.1111/gcb.13205

Withers, P. J. A., & Jarvie, H. P. (2008). Delivery and cycling of phosphorus in rivers: A review. *Science of The Total Environment*, *400*(1), 379–395. doi:10.1016/j.scitotenv.2008.08.002

Wolfe, J. E., & Lind, O. T. (2010). Phosphorus uptake and turnover by periphyton in the presence of suspended clays. *Limnology, 11*(1), 31–37. doi:10.1007/s10201-009-0287-3

Wurch, L. L., Bertrand, E. M., Saito, M. A., Van Mooy, B. A. S., & Dyhrman, S. T. (2011). Proteome changes driven by phosphorus deficiency and recovery in the Brown tide-forming alga Aureococcus anophagefferens. *PLoS ONE, 6*(12), e28949. doi:10.1371/journal.pone.0028949

Yao, B., Xi, B., Hu, C., Huo, S., Su, J., & Liu, H. (2011). A model and experimental study of phosphate uptake kinetics in algae: Considering surface adsorption and P-stress. *Journal of Environmental Sciences, 23*(2), 189–198. doi:10.1016/S1001-0742(10)60392-0

Zhang, H., Davison, W., Gadi, R., & Kobayashi, T. (1998). In situ measurement of dissolved phosphorus in natural waters using DGT. *Analytica Chimica Acta*, *370*(1), 29–38. doi:10.1016/S0003-2670(98)00250-5

Zhao, Y., Chen, X., Xiong, X., & Wu, C. (2019). Capture and release of phosphorus by periphyton in closed water systems influenced by illumination and temperature. *Water, 11*(5), Article 5. doi:10.3390/w11051021

Zięba, D., & Wachniew, P. (2021). Phosphorus transport in a lowland stream derived from a tracer test with 32P. *Water, 13*(8), Article 8. doi:10.3390/w13081030